Universidade do Algarve

Departamento de Medicina e Ciências Biomédicas

Phosphate uptake and phosphate transporter expression during immune cell proliferation in *in vitro* and *ex vivo* leukemic murine models

Andreia Catarina Pereira Afonso

Dissertação de Mestrado

Mestrado em Ciências Biomédicas

Trabalho efetuado sob a orientação de: Professor Doutor Pedro Guerreiro

e Professor Doutor Nuno Santos

Faro, 2015

Universidade do Algarve

Departamento de Medicina e Ciências Biomédicas

Phosphate uptake and phosphate transporter expression during immune cell proliferation in *in vitro* and *ex vivo* leukemic murine models

Andreia Catarina Pereira Afonso

Dissertação de Mestrado

Mestrado em Ciências Biomédicas

Trabalho efetuado sob a orientação de: Professor Doutor Pedro Guerreiro

e Professor Doutor Nuno Santos

Faro, 2015

“Phosphate uptake and phosphate transporter expression during immune cell proliferation in *in vitro* and *ex vivo* leukemic murine”

Mestrado em Ciências Biomédicas

Declaração de autoria de trabalho

Declaro ser a autora deste trabalho, que é original e inédito. Autores e trabalhos consultados estão devidamente citados no texto e constam da listagem de referências incluída.

_____

Andreia Catarina Pereira Afonso

Acknowledgments

Primeiramente agradeço aos meus pais, pela força, confiança, apoio e incentivo que sempre me deram. Sem eles eu não conseguiria ter aceitado esta oportunidade.

Agradeço também aos meus orientadores, Professor Doutor Pedro Guerreiro e Professor Doutor Nuno Santos, por me terem dado esta oportunidade de desenvolver este trabalho sob a vossa orientação. Agradeço igualmente os vossos ensinamentos a mim transmitidos durante este último ano.

A todas as pessoas do Centro de Ciências do Mar e do Centro de Investigação em Biomedicina pela ajuda, colaboração e amizade, em especial à Sandra Silva por me ter ajudado e acompanhado.

Um especial agradecimento às minhas amigas e colegas Rita Nascimento e Filipa Guerreiro. Sem o vosso apoio, a vossa paciência para me ouvir e o nosso ‘embrace’ este ano teria tido menos piada.

Um último, mas não menos importante, agradecimento à Maltinha, pela vossa presença constante na minha vida de sempre e para sempre, e por tentarem compreender a minha ausência nestes últimos meses.

Abstract

Inorganic phosphorus is a mineral found in all human tissues that associated with oxygen, becomes a phosphate anion (PO_4^{3-}). Phosphate is involved in structural and regulatory purposes and its distribution covers soft tissues, extracellular fluids and the large majority is located in skeletal tissues.

Phosphate absorption into the human body is realized by NaPi-IIb cotransporter in small intestine, and its excretion and reabsorption is mediated by NaPi-IIa cotransporter in kidney. This movement into the cell is mediated by SLC34 family and SLC20 family of cotransporters. This family comprehends PiT-1 and PiT-2 proteins that have a housekeeping role in cellular Pi homeostasis. Recently associated with a more specific physiological role, it has been showed their function in bone and parathyroid metabolism and mostly in cell proliferation and mitosis activity.

This work aimed to evaluate tissue localization and expression of SLC20 in mouse model, and attempt to establish functional role of extracellular phosphate and cotransporters in normal and abnormal cell development and proliferation. To accomplish this purpose it were performed quantitative real-time PCR analyses, modulated phosphate availability assays in cell culture and uptake of phosphate assays in leukemic thymic cells.

Altogether, it was confirmed the higher number of cells existent in a leukemic thymus comparing with wild-type. These results suggested that all the phosphate conditions above or below 6 mM resulted in a reduced cell proliferation, being also related with the duration time that cells where exposed to those conditions. It was also shown that intracellular phosphate homeostasis depends only on the amount of phosphate in the extracellular medium, higher the Pi higher the uptake. Lastly, gene expression in different phosphate conditions over time showed that *PiT-1* and *PiT-2* appear to be important for EL-4 cell proliferation, although their specific role was not investigated. Interestingly, XPR1 showed a prospective role as Pi exporter and α-klotho as an aging suppressor.

Keywords: phosphate, SLC20 cotransporters, cell proliferation, thymus and leukemia.

Resumo

O fósforo inorgânico é um mineral essencial encontrado em todos os tecidos e que está normalmente associado com oxigénio sob a forma de anião de fosfato (PO_4^{3-}). O fosfato desempenha diversas funções a nível estrutural, estando incorporado por exemplo no ADN, fosfolípidos e fosfoproteínas. Também executa funções a nível regulador estando envolvido em diferentes mecanismos celulares, como vias de sinalização e crescimento. A sua distribuição abrange os tecidos conectivos e fluídos extracelulares, mas na sua maioria está localizado nos tecidos ósseos.

O fosfato entra no organismo a partir do intestino delgado. Esta absorção é realizada pelo cotransportador NaPi-IIb, e ao mesmo tempo a sua excreção através da urina e a reabsorção é realizada no rim, no túbulo proximal, pelo cotransportador NaPi-IIa. Este simultâneo mecanismo de absorção, excreção e reabsorção mantém o organismo num estado de equilíbrio, com trocas entre o meio intracelular e o fosfato armazenado no meio extracelular. Este estado de equilíbrio é também atingido com a ajuda da hormona paratiroide (PTH), do fator de crescimento fibroblástico 23 (FGF23) e da vitamina D, e quando a sua função e/ou produção fica comprometida pode resultar em diversas patologias.

Este movimento do fosfato para o interior das células é mediado pelos cotransportadores dependentes de sódio acima mencionados que pertencem à família transportadora de soluto SLC34 e também pela família transportadora de soluto SLC20. Esta família é composta por PiT-1 e PiT-2, dois cotransportadores com um vasto padrão de expressão que lhes confere a função de gestores da homeostasia de fosfato a nível celular, mantendo a entrada e saída de fosfato das células contante e de acordo com a necessidade do organismo.

Associada a esta conhecida função de transporte, também existe a hipótese dos transportadores da família SLC20 terem a função de sensores de fosfato tendo em conta as semelhanças com o transportador de fosfato da Escherichia coli e da Saccharomyces cerevisiae. Independentemente da função de transporte, também têm vindo ultimamente a ser estudadas novas funções relacionadas com o metabolismo do osso, com a sua função na paratiroide e por fim a mais importante, com a sua função na proliferação celular e propagação da mitose. Estes últimos estudos foram realizados por Beck e colegas usando a retirada de *PiT-1* que mostrou a repressão da proliferação celular em células HeLa.

Este trabalho tinha como objetivo avaliar os níveis de expressão e consequente localização a nível tecidual, dos genes *PiT-1* e *PiT-2*, da família transportadora de soluto SLC20 no modelo de ratinho. Também outros genes relacionados com transporte de fosfato foram investigados. O *XPR1* que é associado como possível transportador de fosfato no lado basolateral da célula, e o *α-klotho*, recentemente associado com a possível função de anti envelhecimento e supressão tumoral. O trabalho tinha também como objetivo estabelecer a função do fosfato e respetivos cotransportadores no desenvolvimento e proliferação de células normais e tumorigênicas, verificando a diferença nestes dois tipos celulares.

Para realizar estas metas propostas foi efetuada a quantificação por Real-Time PCR dos genes de interesse a partir do ARN extraído de diferentes tecidos previamente recolhidos, avaliando a sua distribuição. De seguida foram realizados ensaios em células em cultura, usando a linha celular EL-4 derivada de linfoma, onde a disponibilidade de fosfato no meio de cultura variava usando as concentrações 0.32 mM, 3 mM, 6 mM, 9 mM e 18 mM. A partir destes ensaios foram estimados o número de células, o uptake de fosfato e a expressão de genes em cada uma das condições de fosfato previamente referidas. Estes ensaios de variabilidade de fosfato também foram realizados em células wild-type e células leucémicas de timo de ratinho.

De uma forma geral, foi confirmada a presença de um maior número de células em timos leucémicos quando comparado com timos wild-type. Ensaios de variabilidade de fosfato sugeriram que a proliferação celular mostra ser reduzida nas condições de fosfato abaixo ou acima do controlo positivo (6mM), apesar dos valores normais no organismo rondarem entre 1.5 e 3 mM. Esta debilitada proliferação também relacionada com o tempo a que as células expostas a estas diferentes concentrações de fosfato, porque quanto mais tempo está na presença das diferentes condições, menor é a proliferação celular.

Foi também verificado que o estado de homeostasia presente no interior da célula deve-se apenas à quantidade de fosfato presente no meio extracelular, porque quanto maior é essa quantidade presente no meio, maior é o seu uptake. Por fim, a expressão de *PiT-1* e *PiT-2* não mostraram variações significativas com as diferentes condições de fosfato, não indicando o seu envolvimento na proliferação celular. Curiosamente, *XPR1* mostrou a possibilidade de estar envolvido no exporte de fosfato, tendo os seus valores de expressão igualado os dos transportadores *PiT-1* e *PiT-2*. α-klotho exibiu uma possível função como agente anti envelhecimento pois apresentou uma expressão mais elevada em células em estado quiescente

do que em células em estado proliferativo. As diferenças de expressão destes mesmos genes não mostrou variação em tecidos wild-type e leucémicos.

Palavras-chave: fosfato, cotransportadores SLC20, proliferação celular, timo e leucemia.

Contents page

Image list

Table list

List of abbreviations

ABC	ATP-binding cassette
AND	Ácido desoxirribonucleico
ARN	Ácido ribonucleico
BBM	Brush border membrane
bp	Base pair
CD	Cluster of differentiation
CDK	Cyclin-dependent kinase
Cpm	Counts per minute
DEPC	Diethylpyrocarbonate
DMSO	Dimethyl sulfoxide
DNA	Deoxyribonucleic acid
dNTPs	Deoxynucleotide-triphosphates
FBS	Fetal bovine serum
FGF23	Fibroblast growth factor 23
Fw	Primer forward
$H_2PO_4^-$	Monovalent phosphate anion
HPO_4^{2}	Divalent phosphate anion
K^+	Potassium
L-Glut	Glutamine
MHC	Major histocompatibility complex
MTT	3-[4,5-dimethylthiazol-2-yl]2,5-diphenyltetrazolium bromide

Na^+	Sodium
$NaHCO_3$	Sodium bicarbonate
PBS	Phosphate-buffered saline
PCNA	Proliferating cell nuclear antigen
PCR	Polymerase chain reaction
PenStrep	Penicillin/Streptomycin
pKa	Acid dissociation constant
PO_4^-	Phosphate anion
RNA	Ribonucleic acid
RT	Room temperature
RTqPCR	Real-time quantitative polymerase chain reaction
Rv	Primer reverse
SEM	Standard error of mean
Ta	Annealing temperature
TRK	Total RNA kit
WT	Wild-type

1. Introduction

1.1 Phosphate in physiological systems

Phosphorus is an essential mineral found in all human tissues[1,2] which plays important roles in many physiological processes, and because of this is very important to maintain its homeostasis. Inorganic phosphorus is usually associated with oxygen in the form of phosphate anion (PO_4^{3-}) that exists predominantly in two forms, the monovalent form $H_2PO_4^-$ and the divalent form HPO_4^{2-}, being that the last embodies 80% of total at a physiological pH of 7.4.[3,4]

Phosphate is involved in structural, metabolic and regulatory processes in every cell. Pi provides the high energy bonds in ATP, is part of nucleic acids and proteins, being therefore incorporated in the DNA structure, in cell membrane phospholipids and in phosphoproteins necessary for mitochondrial function. Phosphate is also important for cellular metabolism, cellular growth, signaling pathways, enzymatic activities via kinase and phosphatase mediated processes and maintenance of acid–base balance.[4–7]

Its distribution is approximately 85% in skeletal tissues complexed with calcium in the form of hydroxyapatite, nearly 15% in soft tissues within cells, and the remainder (less than 1%) spread in the extracellular fluids as inorganic Pi.[4,8–10] It is essential that the extracellular concentration of Pi is maintained at a constant narrow range between 0.8 and 1.5 mM (in humans) for proper cellular function.[4,11]

In humans, phosphate equilibrium is achieved by balancing Pi intake through absorption in the small intestine, exchange with intracellular and body storage pools, Pi excretion in urine, and renal tubular Pi reabsorption in the kidney. The amount of phosphate absorbed across the small intestine is approximately 950 mg/day (Figure 1.1) and represents about 80% of the dietary phosphate. The unbound phosphate existent in the plasma (extracellular pool) is freely filtered by glomeruli and then approximately 90% is reabsorbed in the proximal tubules. In a balanced state, the amount of Pi excreted in urine is almost the same as the Pi absorbed in the small intestine (Figure 1.1).[1,2,12,13]

The movement of Pi into the cell occurs mainly through a process of regulated active transport across the cell membrane, mediated by two solute carrier families of transporters: SLC20 and SLC34 (section 1.2).[4,5,7] These carry both Pi and Na^+, and the transport is partially created by the electronegative charge existent in cell interior relative to the exterior as

consequence of leak in the potassium cation (K^+) channel, which maintains a voltage difference across the cell membrane.[14]

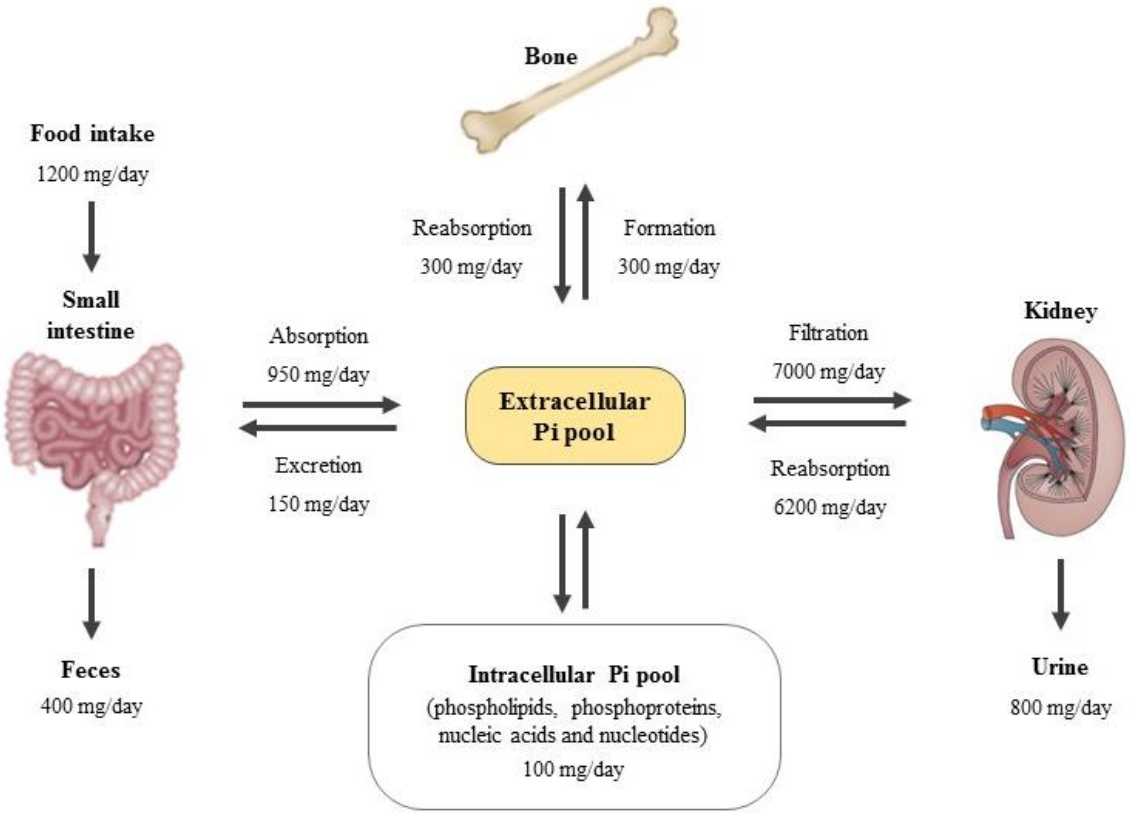

Figure 1.1 – Phosphate homeostasis in humans. The small intestine and kidney play the major roles in phosphate (Pi) homeostasis by regulating absorption and excretion, respectively. In states of neutral Pi balance, most part of Pi absorbed in the small intestine is excreted in urine. The movement of Pi into bone and soft tissues also determines serum Pi concentrations. Exit from extracellular Pi pool into bone formation is roughly equal to entry into the extracellular Pi pool due to bone reabsorption. The same equilibrium process occurs between extracellular and intracellular Pi pool. Adapted from [1,2,12,13]

Concentrations of intracellular phosphate are influenced by pH, hormones, vitamins and subcellular compartmentalization, where the levels in compartments such as mitochondria, lysosomes and endoplasmic reticulum are regulated by separate transporters. The most important regulating hormones are parathyroid hormone (PTH) and FGF23 (fibroblast growth factor 23), and other factors, such as the growth hormone (GH), thyroid hormone (TH) and dopamine, play a secondary regulatory role. These hormones are also denominated

calciophosphotropic hormones because they are dedicated to the regulation of both phosphate and calcium, since the balanced concentrations of these ions are interdependent. Not only is the active form of vitamin D (1,25-dihydroxyvitamin D_3) important for Pi regulation but also metabolic factors and other circulating proteins, which contribute to Pi homeostasis according to the organisms necessities.[1,2,5,7,9,15]

Given the importance of Pi homeostasis, its widespread distribution and critical role in cellular processes it is predictable that its defiance results in severe pathologies. Intracellular phosphate levels are elevated in pathological conditions such as ischemia, hypoxia, skeletal muscle fatigue, and some inherited disorders such as mitochondrial myopathies. Hyperphosphatemia is a common and serious complication of chronic renal failure (CRF), contributing to secondary hyperparathyroidism, tissue calcifications and metabolic changes. Gene mutation can be one of hyperphosphatemia causes as it is also tumoral calcinosis. Conversely, decreased intracellular levels of phosphate are observed in clinical disorders with severe hypophosphatemia and may be caused by malnutrition, malabsorption, or inherited disorders affecting renal phosphate reabsorption such as hypophosphatemic rickets and X-linked hypophosphatemia. Prolonged phosphate deficiency is associated with disruption of both the metabolic and mineralization functions of phosphate leading to osteomalacia, risk of nephrolithiasis, hemolysis, neuropathy, respiratory failure from muscle weakness, and reduced myocardial contractility.[1,15–17]

1.2 Phosphate transporters

Phosphate absorption across the plasma membrane occurs against an electrochemical potential difference, which accumulate phosphate at concentrations larger than would be predicted if phosphate were distributed passively across the membrane. This active process involves the transfer of a phosphate anion from the lumen to cytosol against concentration gradient and therefore can be defined as an active transepithelial transport. Pi import is mediated by secondary-active-Na^+-dependents cotransporters, which rely on a high extracellular sodium gradient, that is maintained by the membrane associated Na^+/K^+ ATPase (Figure 1.2).[18] This cotransporters are located in the apical membrane of the cell and the identity of proteins responsible for the basolateral Pi efflux is still unknown, although recently studies with a

membrane molecule XPR1 may show otherwise.[6] There are two families of solute carriers mainly responsible for the co-transport, which are the SLC34 and SLC20 families (see below).[4,5,18,19] These two families are non-related in their phylogeny and the transporters differ in their amino acid sequence, affinity for phosphate and mechanism controlling their activity and tissue expression.[7] A third cotransporter family, SLC17, is sometimes referred to as type I Na^+-dependent Pi transporter family, but studies using a cloned member of this family in *Xenopus laevis* oocyte showed a low specificity for Pi transport and rather more for transport organic anions, such as glutamate.[20]

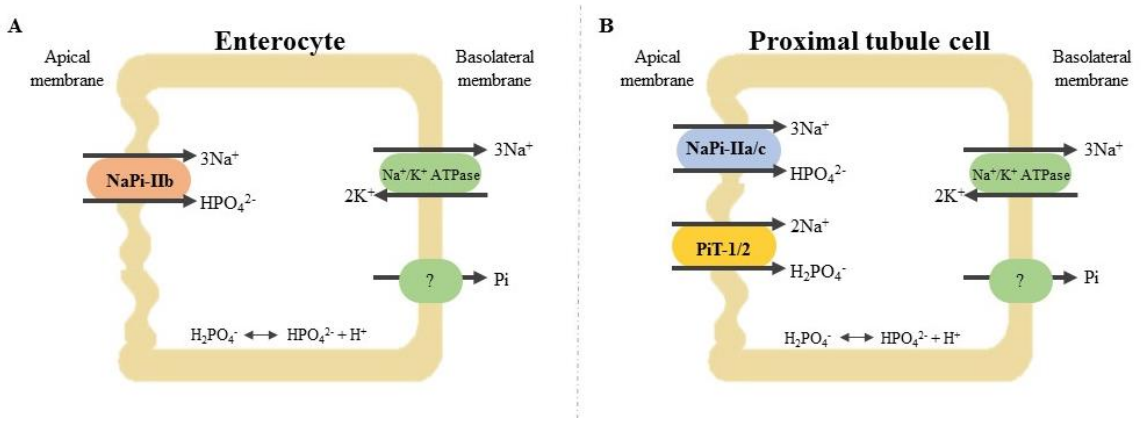

Figure 1.2 – Phosphate transport. Distribution and localization of phosphate transport proteins at the enterocytes in small intestine (A) and at the proximal tubule cells in kidney (B). Pi transport is mediated by Na^+-dependents cotransporters localized in the BBM (apical membrane); (A) NaPi-IIb is responsible for Pi absorption (divalent form,HPO_4^{2-}) in enterocytes and (B) NaPi-IIa, NaPi-IIc (divalent form,HPO_4^{2-}) and PiT-1/2 (monovalent form,$H_2PO_4^-$) are responsible for Pi reabsorption in proximal tubule cells. In both cases this Na^+-dependent co-transport is reliant on Na^+/k^+ ATPase, localized at the basolateral membrane, that conserves a high extracellular sodium gradient. The basolateral Pi exit pathway remains unknown. Adapted from [4,5,21]

1.2.1 SLC34 family

The SLC34 family, referred as a type II Na^+/Pi cotransporter family, includes the three proteins SLC34A1 (NaPi-IIa), SLC34A2 (NaPi-IIb) and SLC34A3 (NaPi-IIc). NaPi-IIa and NaPi-IIc are responsible for Pi reabsorption in the brush border membrane (BBM), a epithelial layer covered with microvilli, of the renal proximal tubules, while NaPi-IIb has broader pattern of expression and it highly abundant in the enterocytes of the small intestine.[4,5,18,22]

All the SLC34 proteins preferentially transport divalent Pi (HPO_4^{2-}) and require Na^+ ions to co-transport Pi, although in a few cases Li^+ ions can also partly replace Na^+ to drive the transport.[23] Both NaPi-IIa and NaPi-IIb are electrogenic and transport divalent Pi, with a strict Na^+:Pi stoichiometry of 3:1. NaPi-IIc is electroneutral and exhibits a 2:1 stoichiometry.[24] The apparent affinity of this transport system for phosphate is 100 µM at 40 mM sodium and pH 7.4.[4] This transport capacity is strongly pH dependent because protons directly modulate the transport kinetics and because pH defines the divalent-monovalent Pi ratio in the lumen, where the acid dissociation constant (pKa) is pH 6,8 in which divalent form (HPO_4^{2-}) turns into monovalent form ($H_2PO_4^-$)[25] Early *in vitro* characterization of this transport used brush-border membrane vesicles (BBMV) from renal and intestinal epithelial tissue[26] and further ones used both cloned transporters in *Xenopus laevis* oocytes to characterize the regulation of the transport.[27] These proteins are the most broadly characterized in terms of function, structure and regulation.[22]

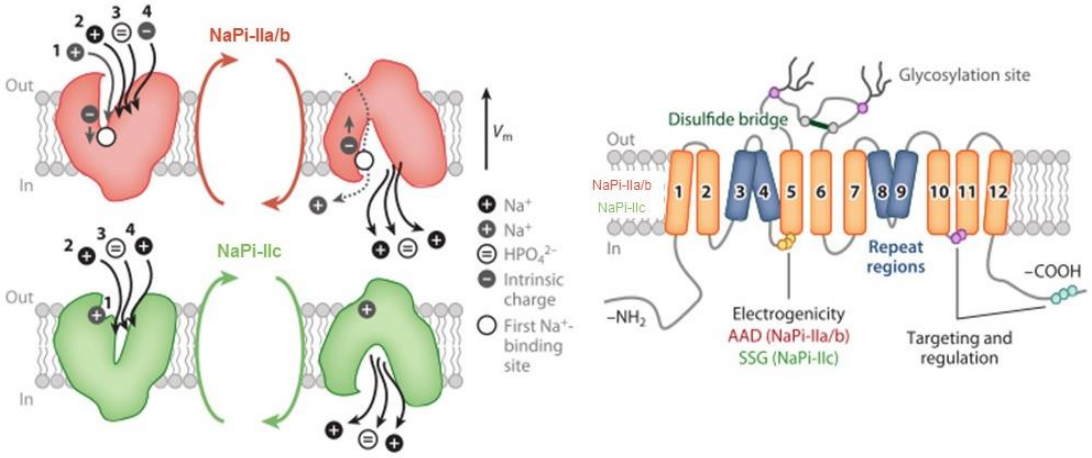

Figure 1.3 – Mechanism and molecular features of SLC32 family. The basic transport cycle is shown in the left panel and the salient molecular features is shown in the right panel. For the SLC34 proteins, the transmembrane protein is inwardly related with Na^+ gradient and comprises an ordered sequence of binding steps (indicated by the numbers) in which two Na^+ ions (1 and 2) bind sequentially, followed by binding of divalent Pi (3) and of a third Na^+ ion (4). Substrate release to the cytosol occurs after reorientation of the fully loaded carrier. For electrogenic NaPi-IIa/b, an intrinsic negative charge (AAD, aspartic acid) confers voltage dependence to the transport cycle, allowing the binding of the first Na^+ ion and subsequent translocation together with the other substrates, giving the 3:1 Na^+:Pi stoichiometry. After all substrates are released to the cytosol, the intrinsic charge again senses the transmembrane field, leading to a voltage-dependent reorientation of the empty carrier. For electroneutral NaPi-IIc, a conserved glycine (SSG) binds one Na^+ ion, like NaPi-IIa/b, but this ion is not translocated, giving a 2:1 Na^+:Pi stoichiometry. Topology model for SLC34 show the predicted transmembrane domains (numbered 1-12) and repeated regions (dark blue). Disulfide bridge, glycosylation sites and critical residues for targeting, regulation, and electrogenicity are highlighted in the right panel. Image adapted from [4,5].

1.2.2 SLC20 family

The SLC20 family, referred as a type III Na^+/Pi cotransporter family is the most recently described one and comprises the proteins SLC20A1 (PiT-1) and SLC20A2 (PiT-2), which are responsible for the transport of the monovalent Pi ($H_2PO_4^-$) with a strict Na^+:Pi stoichiometry of 2:1.[4,5]

This Na^+/Pi cotransporter family was originally identified as retroviral receptors for gibbon ape leukemia virus (Glrv-1)[28] and rat amphotropic virus (Ram-1), a function that was not found in humans.[29] Later to this discover, both receptors were found to mediate phosphate transport in a Na^+-dependent manner after the expression in *Xenopus laevis* oocytes, although the kinetic characterization was very limited. Giving this newly characteristics of the retroviral receptors, Glvr-1 and Ram-1, were renamed PiT-1 (phosphate transporter 1) and PiT-2 (phosphate transporter 2), respectively.[30]

Their widespread expression pattern in all tissues gives them the designation of housekeeping role although more specific physiological roles are emerging for these transporters.[4,5,18,23,31] For example, PiT-1 might play an important role in bone Pi homeostasis and its abundance is regulated by several factors involved in bone metabolism, including BMP2 and IGF-1.[32] Additionally, a number of studies also suggest a role of PiT-1 in hyperphosphatemia induced calcification of blood vessels[33], as well as in parathyroid function.[34] Recently a new function of PiT-1, independent of its transport function, has emerged. Depletion of PiT-1 expression in HeLa cells resulted in reduced cell proliferation and impaired mitosis.[35] In vivo studies accentuated these findings by showing that a PiT-1 knockout mouse is embryonically lethal, reflecting its importance in liver development[36], anemia and arrested growth.[37]

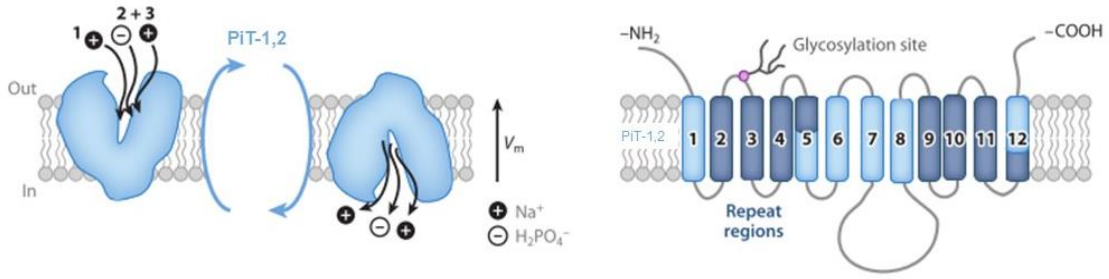

Figure 1.4 – Mechanism and molecular features of SLC20 family. The basic transport cycle is shown in the left panel and the salient molecular features is shown in the right panel. For SLC20 proteins, the transport sequence comprises an initial binding of one Na^+ ion (1), followed by a random interaction of monovalent Pi and a second Na^+ ion (2 and 3). Reorientation of the loaded carrier then leads to substrate release in the cytosol. Topology model for SLC20 show the predicted transmembrane domains (numbered 1-12) and repeated regions (dark blue). Glycosylation sites are highlighted in the right panel. Image adapted from [4,5].

1.3 Phosphate efflux across the basolateral membrane

As described above, phosphate homeostasis in multicellular eukaryotes is dependent on transcellular Pi transport in different tissues and organs, which includes not only controlled Pi influx, but also efflux out of cells. In metazoans, efflux of Pi is an obligatory step at the basolateral side of the kidney proximal tubule and small intestine epithelial cells for Pi transfer to the blood stream. Despite the importance of Pi efflux to its homeostasis, very little is known about its control and the transporters involved in this process.[38]

In mammals, XPR1, a membrane protein initially identified as the cell surface receptor for xenotropic and polytropic murine leukemia retroviruses (X- and P-MLV) has been studied as a possible phosphate exporter given the fact that this protein is homologous with PHO1, responsible for Pi efflux in plants, such as *Arabidopsis thaliana*.[6,38] PHO1 was the first protein to be identified as a Pi export mediator in eukaryotes.[39]

This XPR1 protein reveals a very broad expression pattern in tissues as diverse as kidney, brain, skin, liver, heart and lung,[38] and interestingly, phosphate efflux has also been reported in an extensive range of cells such as pancreatic B cells, hepatocytes, jejunal enterocytes and cells of the renal proximal tubules.[40,41] There are some studies indicating that both XPR1 depletion and blocking with XRBD (X-MLV Env-derived ligand) induced a decrease in Pi export and that reintroduction of various XPR1 proteins, from fruit fly to human, restored this deficiency.[6] Altogether, these data suggest that although alternative pathways for

phosphate export may exist, the severity of its inhibition indicate that XPR1 has an important physiological role in controlling phosphate.[38]

1.4 Regulation of phosphate absorption and/or reabsorption

Body phosphate homeostasis is largely dependent by modulation of intestinal absorption of dietary phosphate, renal phosphate reabsorption and excretion, and the exchange of phosphate between extracellular and bone storage pools.[2] Serum levels are regulated by a combination of local and humoral factors. The majority of this humoral factors are calciophosphotropic hormones including parathyroid hormone (PTH), fibroblast growth factor 23 (FGF23), active vitamin D (1,25-dihydroxyvitamin D_3), among others factors, that are maintained by several negative feedback loops.[42,43]

1.4.1 Small intestine

As described previously, the phosphate absorption is executed in the small intestine and its Na^+-dependent transport in the brush border membrane of enterocytes is mediated by NaPi-IIb (Figure 1.5) and it provides the rate-limiting step for the transcellular uptake of Pi[44,45]. Studies using NaPi-IIb knockout mice have shown that absence of this intestinal brush border membrane transporter triggers compensatory renal mechanisms where, NaPi-2a is upregulated, to maintain phosphate homeostasis[46] suggesting that phosphate balance is mediated at a central level.

There has also been interest in the potential role of PiT-1 and PiT-2 in intestinal phosphate transport. A recent study revealed that *PiT-1* mRNA is present throughout the small intestine, while the mRNA levels of *PiT-2* are low. Both these proteins may contribute only moderate (approximately 5%) to transepithelial Pi transport in small intestine.[5,45]

Dietary phosphate and vitamin D are thought to be the most important physiological regulators of intestinal Pi absorption.[47] Vitamin D will enhance *NaPi-IIb* expression as described in Figure 1.5. There are other factors as glucocorticoids,[48] estrogens and metabolic acidosis[49] that can also affect intestinal absorption.

1.4.1 Kidney

Following absorption in the small intestine, Pi reabsorption in the kidney is the next, and most well-known step, to maintain Pi homeostasis. The Na^+-dependent phosphate transport in the brush border membrane of proximal tubule is mediated by NaPi-IIa and NaPi-IIc, which act as the rate-limiting step for phosphate reabsorption of filtered phosphate from urine.

Interestingly, even though double knockout mice for *NaPi-IIa* and *NaPi-IIc* presented severe hypophosphatemia and increased phosphaturia, there is still residual renal phosphate reabsorption which indicates that there are others transporters able to maintain some Pi reabsorption. In this situation, *PiT-1* and *PiT-2* mRNAs were detected in the kidney, but only PiT-2 occurred as protein.[16] As in small intestine, PiT-1 and PiT-2 appear to only contribute with 5% to transepithelial transport in kidney in normal conditions.[5]

Renal Pi reabsorption is regulated by dietary Pi intake and several hormones, such as PTH, vitamin D and FGF23, that can directly or indirectly control Pi balance (Figure 1.5).[50] In addition there are other minor hormones that also affect renal Pi handling for example growth hormone, insulin and thyroid hormone can increase phosphate reabsorption, whereas calcitonin and glucocorticoids can decrease it.[3] PTH is the most powerful phosphaturic hormone,[51] and its production is enhanced by high circulating phosphate levels[42], suppressing Pi reabsorption by inducing NaPi-IIa internalization and subsequent lysosomal degradation (Figure 1.5).[52]

FGF23 is a bone derived phosphaturic hormone secreted by osteocytes and osteoblasts[53] and its effects are mediated by binding to FGF receptors (namely FGFR-1) and co-receptor α-klotho.[54,55] FGF23 is a circulating hormone and its signaling inhibits renal Pi reabsorption by suppressing the expression of NaPi-2a cotransporter and Pi absorption by inhibiting PTH activity and vitamin D synthesis.[3,56]

α-Klotho is a newly identified membrane protein, characterized as an anti-ageing gene and a tumor suppressor.[57,58] Genetic mutation of klotho in mice causes premature aging-like phenotypes such as vascular calcifications and skin atrophy. Its overexpression suppresses aging and extends lifespan and at the same time that it may result in inhibited cancer cell proliferation.[57,58] α-Klotho is predominantly expressed in renal distal tubules[59] where it plays its main function as a co-receptor of FGFR regulating FGF23 signaling and so contributing to Pi homeostasis. It is also known that α-klotho can regulate Pi excretion independent from FGF23 as paracrine and endocrine mediator, when under the form of soluble klotho.[55] Studies

in a α-klotho knockout mice and a FGF23 knockout mice indicate increased renal expression of the NaPi‑IIa protein and elevated serum levels of vitamin D, associated with hyperphosphatemia.[60]

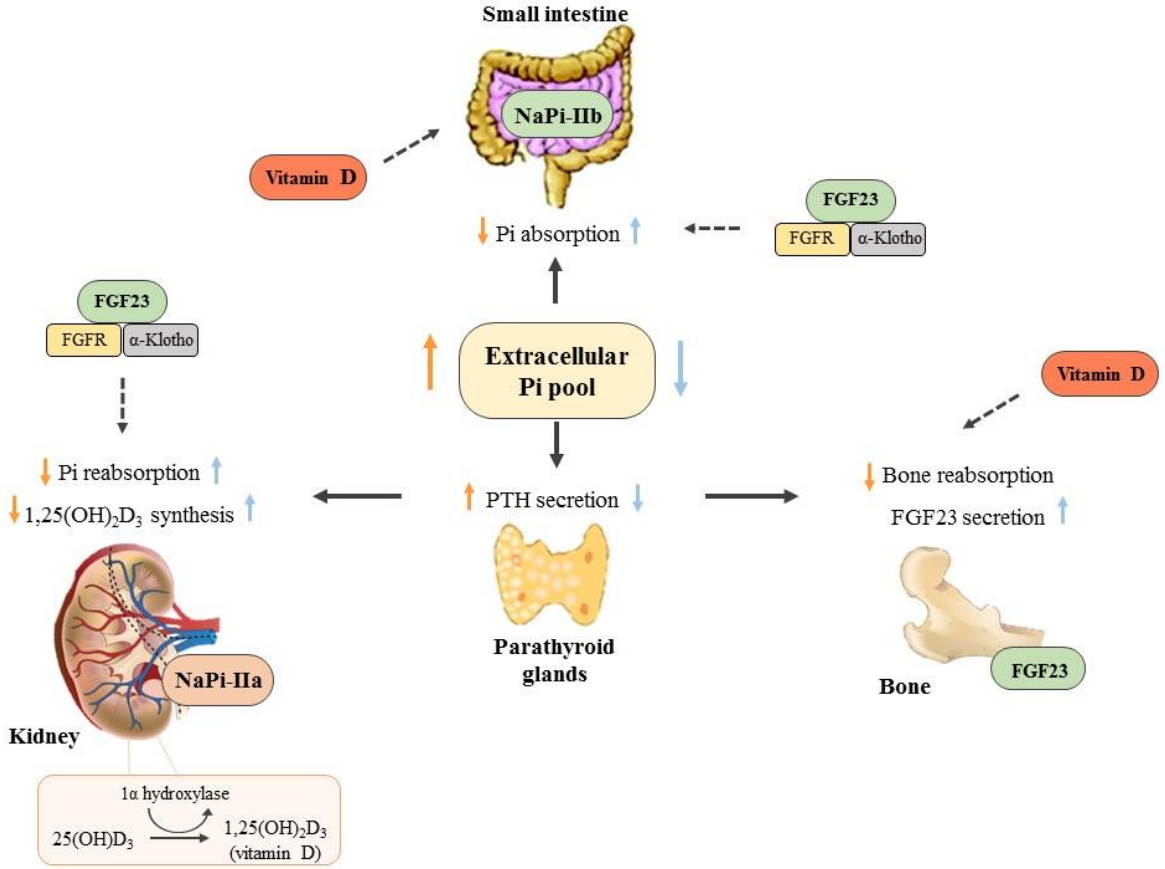

Figure 1.5 – Phosphate regulation. Phosphate is mostly regulated by dietary Pi intake, PTH, 1,25-dihydroxyvitamin D_3 (vitamin D active form) and FGF23, that can directly or indirectly control Pi balance. When Pi uptake is elevated, the extracellular Pi pool is increased, and to try normalize this hyperphosphatemia state, parathyroid glands are enhanced to secrete PTH that will act on the kidney and reduce Pi reabsorption mediated by cotransporter NaPi-IIa, and it will also reduce the synthesis of active vitamin D by inhibiting the enzyme that mediates this synthesis, 1α hydroxylase. As consequence, Pi absorption in the small intestine mediated by the cotransporter NaPi-IIb, is also reduced, given the fact that this is enhanced by vitamin D. In addition, Pi reabsorption in bone will also be inhibited. In cases of hypophosphatemia, the reverse of what was described above will occur. In this state, FGF23 production by osteocytes and osteoblasts in bone and consequent secretion will increase, which is also enhanced by active vitamin D up-regulation. FGF23 acts through one or more FGF receptors, with Klotho as co-receptor, to reduce renal phosphate re-absorption, to decrease circulating vitamin D levels. Adapted from [17,61].

1.4.2 Phosphate sensing mechanism

A diversity of mechanisms have evolved to maintain phosphate homeostasis. In cases of phosphate deficiency, acquisition and retention of Pi by the organism should be accelerated, and contrariwise, in cases of Pi excess, acquisition and retention of Pi should be reduced. A necessary first step in Pi regulation is the ability of a cell or organism to sense changes in Pi concentrations in its environment and adjust its metabolic processes to accommodate such variations. Phosphate sensing in bacteria, such as *Escherichia coli*, and yeast, as *Saccharomyces cerevisiae*, appears to involve uptake of extracellular phosphate, activation of an intracellular sensor which leads to the transcription of phosphate-specific proteins. Based on these considerations it is possible that similar events are conserved in metazoan species including humans, however the exact molecular nature of these mechanisms is still unclear.[1,17,23,62]

In *Escherichia coli*, when the phosphate specific transporter "detects" low Pi concentrations in the environment, the Pi retention will increase. This process is achieved by a sequence of phosphorylation reactions of a regulatory system that interacts with a "phosphate regulon", a collection of genes under regulation by the same regulatory protein, being the predominant Pi uptake system. Bacteria express a second family of phosphate transporters, which are related to eukaryotic type III sodium-phosphate cotransporters (SLC20) but they serve primarily as a cotransporter of divalent metal cations associated with phosphate. Interestingly, PhoU, a protein integrated in the phosphorylation reactions described above, contains a domain similar to eukaryotic type II sodium-phosphate cotransporters (SLC34), but the significance of which is unclear.[17]

In *Saccharomyces cerevisiae*, phosphate controls a specialized transcription factor called Pho4, and the reduced Pi concentrations in the external environment results in its inactivation by the complex Pho80-Pho85. The inactivated Pho4 will enter the nucleus and bind to Pho-regulon including genes for high affinity phosphate transporters (Pho84 e Pho89).[63] This phosphate transporter Pho84 belongs to a large family, which includes the type I sodium-phosphate transporters (SLC17) and Pho89 is related to both member of type III sodium-phosphate transporters family (SLC20).[17]

Additional studies of phosphate-sensing made by Markovich et al using kidney epithelial cells from opossum showed that they are able to respond to changes in environmental Pi concentrations by altering the efficiency of Na^+-dependent Pi absorption in a short time, after 2 h of cell culture.[64] In addition it was shown that non-epithelial cells, such as osteoblastic,

fibroblastic and marrow stromal cell have a response to changes in environmental Pi concentrations by altering BMP-4 (bone morphogenic protein 4) expression, *Runx2/Cbfa1* (transcriptions factor regulators of bone formation) localization, alkaline phosphatase secretion and MAPK signaling pathway Pi activation dependency. Additionally, blocking PiT-1 co-transport receptor showed an inactivation of MAPK signaling pathway that in agreement with the previous data suggest a sensorial detection mechanism.[1,17]

Phosphate regulation in animals have suggested that immediately following a meal containing Pi, rapid alterations in the renal excretion of phosphate occur that are not associated with changes in calciophosphotropic hormones, such as vitamin D and PTH, and other regulating factors. However, the feeding of animals with high Pi diets over a period of weeks shows changes in the regulatory factors, suggesting that this sensing detection mechanism may be related with the short-term response to alteration of phosphate concentration.[62] Segawa et al have demonstrated an increase in NaPi-IIb expression in vitamin D receptor knockout mice[65] but in contrast, the amount of *PiT-1* mRNA was increased and only decreased after administration of vitamin D[34], strengthening the existence of a sensor within or in the surface of cells that is able to detect changes in the concentration of phosphate.

There are only sparse examples in the literature of transporters or channels that have been shown to possess additional functions independently of their transport function. Additionally to the ones showed above, Human PiT2 has been shown to modify its oligomerization independently of Pi uptake in response to changes in the extracellular Pi concentration, suggesting a possible role of PiT2 in Pi sensing. However, it is not known whether PiT-2 (or PiT-1) has any direct signaling activity in response to Pi. A potential role of PiT proteins in Pi sensing maybe important for cellular functions, such as proliferation.[66]

1.5 Role of Pi in cell development and proliferation

The SLC20 family includes two proteins PiT-1 and PiT-2 with a known function in phosphate transport, as described previously. Their broad tissue distribution has led to the proposal that these two cotransporters could perform a housekeeping role for cellular Pi homeostasis.[4,31,67] In contrast with the SLC34 family of cotransporters, which have been extensively explored and characterized,[11,68] the novel roles, in addition to Pi transport, of these

ubiquitously expressed SLC20 proteins only beginning to emerge.[67] Given the combined role of phosphate in cellular processes and the function of PiT-1 and PiT-2 as ubiquitous suppliers of phosphate to the cell, it was not unexpected to uncover a new role for these transporters may have additional roles in bone metabolism[69], parathyroid function[34] and most importantly in cell proliferation and mitosis activity[35,70] independent from the already known transport function.

Bone is a major organ involved in Pi homeostasis and its storage, so Pi systemic control is indispensable for bone formation and mineralization.[61] Yoshiko et al showed that a Na^+/Pi cotransporter inhibitor blocked the mineralization of cultured osteoblasts, and the same was true for local mineralization in newborn rats skulls after injection. Gene expression of both *PiT-1* and *PiT-2* decreases along osteoblast development, where *PiT-1* expression is higher than *PiT-2*, but conversely the accumulation of respective proteins increases with development. This information coupled with the fact that these researchers showed a higher necessity of Pi in mature osteoblast suggests that both PiT-1 and PiT-2 may play a different roles in bone tissue.[69]

High levels of phosphate are associated with hyperphosphatemia, and are also important in the development of hyperparathyroidism, which is characterized by an increase in parathyroid cells number and consequent PTH production. Currently there is no evidence that the uptake of extracellular Pi is necessary to exercise its effect on PTH. Moreover, Tatsumi et al showed that the Pi action may be mediated by PiT-1, not as a Na^+/Pi cotransporter but as a cell surface Pi-sensing protein[34] in bacteria and yeast.[17]

Recent studies have shown that *PiT-1* depletion repressed cell proliferation in HeLa cells[35] and that *PiT-1* knock-out mice did not survive past day 12.5 of development (E12.5)[36]. In HeLa cells it was observed that *PiT-2* overexpression partially recovered the defective PiT-1 transporter function, and Pi uptake reached almost normal levels, but did not rescued the cell proliferation defects. These findings are consistent with the knock-out mice results where E11.5 embryos with *PiT-1* mRNA levels below 15%, comparing to the wild-type (WT), showed an up-regulated *PiT-2* expression, indicating that compensatory elevated *PiT-2* expression is essential for survival of *PiT-1*-deficient cells. It is also important to highlight that *PiT-1* knock-out mice at E11.5 showed a reduced proliferation of developing hepatocytes and subsequent reduced hematopoiesis. Given the fact that Pi uptake was not altered significantly in any of the previous cases and that cell proliferation was not rescued by *PiT-2* indicates that the transport function of PiT proteins is independent from this newly hypothesized function as cell proliferation regulators.[35] Differences in function/recovery in rescued systems may also be

explained by the only 75% homology between this two proteins. PiT-1 has a intracellular loop not shared with PiT-2 and other members of the SLC20 family in plants and bacteria.[71]

It was also described that over-expression of *PiT-1* can increase the proliferation and the culture densities of two cell lines, MC3T3-E1 and NIH3T3. These cell lines exhibit strictly density-inhibited cell proliferation, indicating that *PiT-1* not only is involved in cell proliferation but can also regulate cell density and anchorage-independent growth.[70]

On the steps of this published data showing that SLC20 family proteins, especially PiT-1, are involved in proliferative and development cellular processes, this project will take advantage of the highly proliferative thymus to further try to understand these mechanisms, using tumorigenic cell lines and isolated cells from normal and abnormal tissue, namely from thymic lymphoma cells.

The thymus is a small organ composed by two lobes located in the thoracic cage just behind the sternum. The thymus is an important part of the body's immune system and is involved in the production and maturation of T lymphocytes. T lymphocytes develop in the thymus (Figure 1.6) and then exit, through the blood circulation, colonizing different tissues including secondary lymphoid organs (e.g. spleen and lymph nodes) and the bone marrow, where they will exert their immune function. There they help the immune system to protect the body from viruses, fungus, other types of infections, and malignantly transformed cells.[72,73] As the thymus is composed of different cell types, each can develop into different types of cancer. Epithelial cells originate thymomas and thymic carcinomas, while neuroendocrine cells originate carcinoid tumors and lymphocytes lymphomas.[74]

Tumorigenic cells are well known for sustaining proliferative signaling, abnormal cell growth, resisting cell death, enabling replicative immortality and enhanced proliferative rate[75] which are the ideal characteristics to evaluate the role of phosphate and transporters in cell development and proliferation.

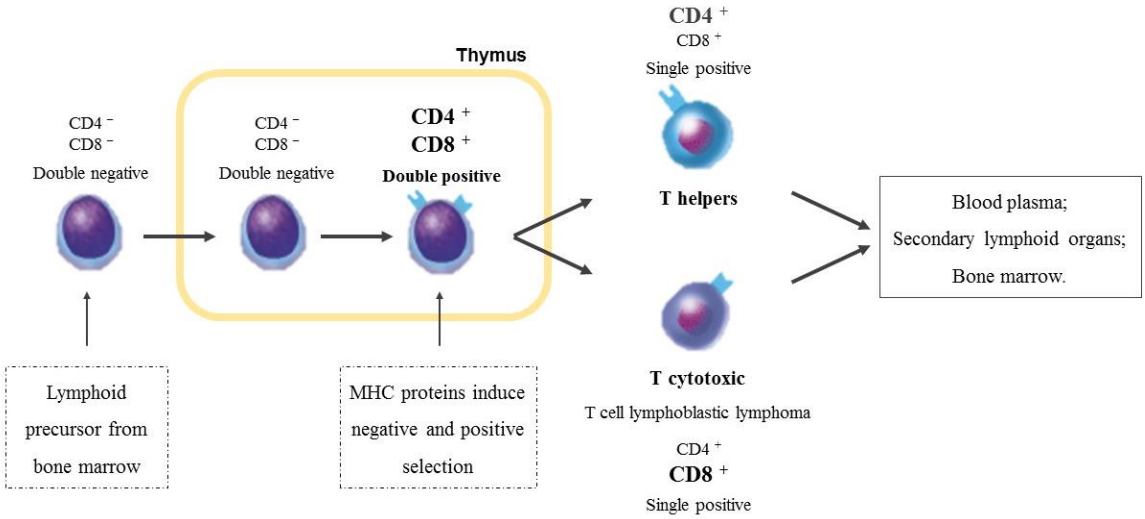

Figure 1.6 – T cell maturation diagram. T cells precursors from the bone marrow enter the thymus through the blood circulation to undergo further maturation. In an early stage, inside the thymus, they are double negative for CD4 and CD8 (membrane glycoproteins that act as cluster of differentiation) until MHC proteins (major histocompatibility complex) enhance a negative or positive selection, and maturation towards either CD4 or CD8 single-positive T cells. T helper cells are single positive for CD4 and T cytotoxic cells are single positive for CD8. Important to notice that leukemic cells in lymphoblastic lymphomas also express CD8 proteins. Upon maturation they then leave the thymus to enter blood circulation and consequently other tissues, such as secondary lymphoid tissues. Adapted from [72,73].

1.6 Objectives

Phosphorus an essential mineral found in all human tissues and is involved in structural, metabolic and regulatory purposes in every cell such as cellular metabolism, cellular growth and signaling pathways. Pi homeostasis is maintained through transepithelial transport that is secured by SLC34 and SLC20 family in the apical membrane and possibly by XPR1 in basolateral side of the cell. Novel functions have been suggested for the SLC20 family, regarding cell proliferation and Pi-sensing, that may be relevant for the control of pathological conditions. Thus it is important to better understand its function in the organism the relations with associated proteins.

The objective of the present study was to evaluate the role of extracellular phosphate in cell proliferation and the involvement of SLC20 members during this process. Consequently, tissue localization and expression levels of cotransporters PiT-1 and PiT-2, and related genes in mouse model were characterized in an attempt to establish its functional roles and involvement in normal and abnormal cell development and proliferation. To this end were used a lymphoblastic derived cell line (EL4), and wild-type and leukemic thymic cells removed from mice. To accomplish these goals, a methodology involving cell culture, mouse breeding and sampling, molecular biology and ^{33}Pi transport assays was followed.

2. Methodology

2.1 Cell culture

The EL-4 cell line was used for *in vitro* experiments. This cell line was established from a mouse thymic lymphoma, and therefore belongs to the T cell lineages.

The EL-4 cell line was culture in suspension in RPMI 1640 (LONZA) cell culture medium supplemented with 10% fetal bovine serum (FBS, Biowest), 1% Penicillin/Streptomycin (LONZA) and 1% Glutamine (Sigma-Aldrich). Subcultures were maintained within a concentration of 2-20x10^6 cells/ml in T-25 or T-75 flasks, according to the experimental needs, in an incubator (Heracell™ 150, Thermo-Scientific) at 37ºC in a humidified 5% CO2 atmosphere. The cell culture medium was renewed every 2 to 3 days by adding or replacing with fresh medium, depending on the cell culture density and medium saturation.

2.1.1 Proliferation assay in serum starvation

Cells were seeded in 100 mm diameter Petri dishes in triplicate at a concentration of 2,5x10^5 cells/ml in RPMI 1640 standard growth medium with two different FBS concentrations: 0.1% and 10%. At 24h, 48h and 72h time-points, the cells were resuspended and an aliquot of each condition and replicate was diluted 1:1 in Trypan Blue solution 0.4% (Sigma-Aldrich) and counted using Neubauer counting chamber (MARIENFELD). At the 48h time-point cells from both conditions were centrifuged (Eppendorf) at 500g for 5 minutes and resuspended in RPMI 1640 standard growth medium with 10% FBS to evaluate cell recovery from a quiescent state. In every time-point, an aliquot of 1x10^6 cells was collected at each experimental replicate that were combined as a single sample, for posterior RNA extraction and molecular analysis. Every sample was stored in RNAlater as described below. All experiments were performed in triplicate.

2.1.2 Proliferation assay in phosphate starvation

Cells were seeded in 24-well plates at a concentration of 2.5x10^5 cells/ml in RPMI 1640 without phosphate, with 0.85 g/l sodium bicarbonate ($NaHCO_3$) supplemented with 10% FBS,

1% Pen Strep, 1% L-Glut and 13,69 mM/L $NaHCO_3$, to match the RPMI 1640 standard growth medium pH values.

Cells were cultured in different phosphate conditions where a different amount correspondent to these concentrations was added from a phosphate Sorensen buffer 0.5 M stock solution (annex 1): 0.32 mM (residual Pi concentration present in the cell culture medium); 3 mM; 6 mM; 9 mM and 18 mM, for 96h, using as positive control cells cultured in RPMI 1640 standard growth medium (≈ 6 mM PO_4). At 24h, 48h, 72h and 96h time-points, the cells were resuspended and an aliquot of each condition and replicate was diluted 1:1 in Trypan Blue solution 0.4% (Sigma-Aldrich) and counted using Neubauer counting chamber (Marienfeld).In every time-point an aliquot of $1x10^6$ cells was collected for every technical replicate at each experimental replicate that were combined as a single sample, for posterior RNA extraction and molecular analysis. Every sample was stored in RNAlater as described below. All experiments were performed in triplicate.

2.1.3 Cell viability assay for cytotoxicity evaluation

Cells were seeded in 96-well plates at a concentration of $1x10^4$ cells/well in RPMI 1640 without phosphate (described above), and cultured in different phosphate concentrations: 0.32 mM; 3 mM; 6 mM; 9 mM and 18 mM for 48h and 96h, in separate plates, using as positive control cells cultured in RPMI 1640 standard growth medium (≈ 6 mM PO_4).

At the end of the assay, at 48h or 96h, 10 µl of MTT solution (5mg/mL in PBS) was added to each well and incubated at 37ºC for 4h. MTT (3-[4,5-dimethylthiazol-2-yl]2,5-diphenyltetrazolium bromide) is a yellow substrate that is cleaved by living cells to produce a dark blue formazan product, a process that requires active mitochondria.[76] At the end of the incubation 100 µl of DMSO (Dimethyl sulfoxide, Sigma-Aldrich) was added to dissolve the formazan to give a homogeneous blue solution suitable for absorbance measurement. After 1h of incubation, the absorbance was measured on a spectrophotometer plate reader (Infinite® M200, Tecan) at a wavelength of 570 nm. All experiments were performed in triplicate.

2.1.4 Phosphorus quantification assay

The phosphorus quantification was determined by means of a phosphorus colorimetric assay (ref. 1001155, Spinreact) modified for microplates. Concentration was measured in samples collected at three time-points of cell culture: 0h, 48h and 96h, using the culture medium with different phosphate levels in the section 2.1.2. At 0h the samples were collected prior to phosphate addition to cells, and at 48h and 96h the samples were collected from the cell culture by centrifugation at 500g during 5 minutes. Briefly, a standard curve was prepared with a range of 0 mM to 7.5 mM from the $Na2HPO_4$*NaH_2PO_4 (Sodium hydrogen phosphate* Sodium dihydrogen phosphate) stock solution provided in the assay Kit. Next, 2.5 µl of each standard point and the same volume from each sample were plated in a 96-well plate, with three technical replicates each. Then after incubation for 10 minutes at RT, the absorbance was measured on a spectrophotometer plate reader at a wavelength of 340 nm.

2.1.5 Phosphate uptake assay with ^{33}P

Phosphate measurements were performed for cells that were submitted to the conditions described in section 2.1.1 and 2.1.2. For the serum starvation, ^{33}P was measured in cells collected at two time-points of culture, 48h and 72h, while in the phosphate starvation ^{33}P was measured at 96h.

After the cultivation period cells were collected in 4 replicates of $1x10^6$ cells each for every condition. Cells were then incubated with approximately 0.063 µl of the ^{33}Pi radioisotope (specific activity: 5 µCi/µl) solution, diluted in RPMI 1640 culture medium in a total of 500-1000 µl (standard for 2.1.1 and without phosphate for 2.1.2). A preliminary assay was carried out on both conditions to determine the kinetics of Pi uptake over time. Samples were collected at 0, 5, 15, 30 and 60 minutes after the incubation with the radiotracer. In all situations it was found that close to linear uptake (measured as decays per minute inside the cells as indicated below) occurred between 0 and 30 minutes, with a plateau period following from 15 to at least 6 minutes (Figure 3.6A).

Therefore the subsequent incubations were performed in two time-points, 5 and 30 minutes, at 37ºC. After the incubation, cells were immediately centrifuged at 500g for 5 minutes at 4ºC and washed two times with respective cell culture medium without tracer. The precipitated cells were then resuspended in 300 µl PBS and pipetted to a scintillation vial.

Following the addition of liquid scintillation (3.5 ml) the beta radioactive energy emitted from inside the cells was determined as counts per minute (approximation to decays per minute) by counting each sample for 10 minutes in a Microplate Scintillation and Luminescence Counter (MicroBeta TriLux, PerkinElmer). All experiments were performed in triplicate.

2.2 Mouse breeding and sampling

The wild-type mice used for tissue expression studies were from the inbred strain C57BL/6. For the remaining studies the TEL-JAK2 transgenic animals[77] were also used. The C57BL/6 strain is the most well-known inbred mouse strain with the entire genome published, and has been widely used as a genetic background for congenic and mutant mice. The TEL-JAK2 transgenic mice results from a chromosomal translocation initiated with the fusion of *JAK2*, a gene on chromosome 9p24 to *TEL*, a gene localized at 12p13 that will encode a chimeric protein, TEL-JAK2, that contributes to the development of acute lymphoblastic leukemia.[77,78]

For tissue expression analysis two males and one female wild-types mice were randomly chosen. Mice were euthanized by carbon dioxide inhalation followed by cervical displacement, and then placed on a flat surface, sprayed with ethanol and dissected. Dissection was initiated with a small abdominal incision that was gradually increased until whole abdominal cavity was exposed, followed by the removal of the tissues of study.

2.2.1 RNA expression studies

The dissection and extraction material was cleaned with RNaZAP (Sigma; spray solution that destroys superficial RNases) to prevent RNA degradation, and a sample of each tissue (about 0.5 cm^3 each) was stored in RNAlater (Sigma; solution that stabilizes and protects RNA at RT by rapidly penetrating the tissue). Samples were initially stores at 4ºC for 24 hours and then at -20ºC according to the manufacturer's instructions until further processing. RNA extraction was performed with an E.Z.N.A. ® Total RNA Kit I (VWR) following the protocol described in the kit instructions as indicated in the sections below.

2.2.2 Cell collection and culture

For the assays with variation of phosphate availability, a total of 6 animals, 3 wild-type and 3 leukemic, were sacrificed using the same method as previously described. Leukemic animals usually present slower locomotion movements as well as slower reaction to human handling due to general weakness. They also present overweight that are associated with the evident swelling of the thymus, spleen and lymph nodes. Upon dissection, these characteristics were observed and presence of leukemic cells was confirmed using cell surface fluorescent immunostaining for flow cytometry.

The thymus was recovered and maintained in ice-cold PBS 1X until cell extraction. Cell extraction was performed using a cell strainer against which the tissue was disintegrated with a syringe piston. The strainer was washed with RPMI 1640 medium with β-mercaptoethanol in a dilution of 1:1000 (helps to preserve the cell membrane), the cells were recovered in a 50 ml conical tube and after adding Trypan Blue solution 0.4% (Sigma-Aldrich) diluted 1:1, counted in a Neubauer counting chamber (Marienfeld), for following molecular analysis, immunostaining and ^{33}P uptake assay.

2.2.3 Cell surface fluorescent immunostaining for flow cytometry

After thymus recovery from sick mice, and to confirm the presence of leukemic cells, I used a technique of immunostaining where membrane cluster of differentiation proteins are recognized by specific fluorochrome-labeled monoclonal antibodies.

Table 1 – Specific murine antibodies used in FACScalibur flow cytometry with fluorochromes PE (R-phycoerythrin) and Cy5 (cyanine).

Antigens	Specie	Primary antibody	Fluorochrome	Emission spectra (nm)	Dilution
Anti-CD4	Murine	Rat IgG2b, k	PE	578	1/400
Anti-CD8	Murine	Rat IgG2a, k	PE/Cy5	667	1/800

For cell surface immunostaining assay, I used $1x10^6$ cells for each sample. For the two thymic cell types (WT and leukemic) one tube was prepared without antibodies, one tube with each antibody, to assess overlap of emission spectra in the flow cytometer, and one with the

two antibodies (see Table 1). To each tube 1 ml of cold PBS/3%FBS/10 mM NaN_3 was added and then centrifuged at 300g for 5 minutes at 4ºC. After discarding the supernatant, the pellet was resuspended in PBS/3%FBS/10 mM NaN_3 with each antibody in a final volume of 50 µl for 1h on ice in the dark. To stop the incubation, 1 ml of PBS/3%FBS/10 mM NaN_3 was added and centrifuged at 300g for 5 minutes at 4ºC. This step was repeated and the cells finally resuspended in 1 ml of PBS/10 mM NaN3 before analysis in a FACSCalibur (Becton Dickinson) flow cytometer. A total of 10 000 events were acquired and analyzed using the CellQuest software (Becton Dickinson).

2.2.4 Phosphate uptake measurement assay with ^{33}P

Phosphate uptake measurements were performed in T cells right after tissue and cell recovery. Preceding the assay uptake, the cells were maintained at 37ºC for 1h in two conditions: RPMI 1640 medium with or without phosphate. For each condition 4 replicates of $1x10^6$ cells were collected. Cells were then incubated with approximately 0.063 µl of the 33Pi radioisotope (specific activity: 5 µCi/µl) solution, diluted in the correspondent RPMI 1640 culture medium as described above. This incubation was performed in two time-points, 5 and 30 minutes, at 37ºC. After incubation, cells were immediately centrifuged at 500g for 5 minutes at 4ºC and the culture medium in the supernatant removed. Cells were resuspended and the procedure repeated to wash the cells twice in cell culture medium without radioisotope. As described above, after the last wash cells were resuspended, transferred to scintillation vials and upon the addition of scintillation cocktail (ref. 1200-434; PerkinElmer), the radioactivity of each sample was measured for 10 minutes in a Microplate Scintillation and Luminescence Counter (MicroBeta TriLux, PerkinElmer). Liquid scintillation is a chemical that incorporates the radiolabeled compound allowing a uniform distribution and capable of converting the kinetic energy of nuclear emissions into light energy. All experiments were performed in triplicate.

2.3 Molecular Analyses

To evaluate expression of the phosphate transporter and associated genes mRNA was isolated and then complementary DNA (cDNA) synthetized and at last a polymerase chain reaction (PCR) or real time polymerase chain reaction (RT-PCR) was performed using specific primers.

2.3.1 RNA extraction and quantification

RNA extraction was performed using the Total RNA Kit I (VWR) for tissues and TRI Reagent for cell pellets.

Extraction of RNA with E.Z.N.A. ® Total RNA Kit I (Omega, VWR) was performed following the provided protocol. First the amount of sample that would be used for the extraction was determined. Then TRK Lysis Buffer with β-mercaptoethanol 14.3 M was added to the sample to disintegrate the cellular membrane. This mixture was homogenized, centrifuged at 13200g for 10 minutes and the obtained supernatant was transferred to a new microtube. Next, 70% ethanol was added to the supernatant and mixed by repeated tube inversion to precipitate the RNA. This solution was transferred to a HiBind RNA column in a collection tube and then centrifuged at 10000g for 1 minutes at RT. The supernatant was discarded and then RNA Wash Buffer I was added to the column and centrifuged at 10000g for 1 minutes at RT, following the same steps with RNA Wash Buffer II (with previously added absolute ethanol). RNA was eluted by adding DEPC (diethylpyrocarbonate) water (see annex 1) in the column and centrifuging at 13200g for 2 minutes. RNA was stored at -20ºC. DEPC treated water is used to inactivate RNase enzymes by the covalent modification of histidine, lysine, cysteine, and tyrosine residues.

Extraction of RNA with TRI Reagent (Sigma-Aldrich) was prepared following the provided protocol. First, 1 mL of TRI Reagent was added to the cell pellet, then gently vortexed and incubated for 5 minutes at RT. Next it 200 µl of chloroform were added to precipitate the RNA, incubated for 5 minutes at RT, mixing occasionally, and then centrifuged at 12000g for 10 minutes at 4ºC. The supernatant was transferred to a new eppendorf tube, 500 µl of isopropanol were added and incubated for 5 minutes at RT. Then centrifuged at 12000g for 10 minutes at 4ºC, and the supernatant was discard. Next 1 ml of 75% ethanol was added, and the

solution was vortexed and centrifuged at 7500g for 5 minutes at 4ºC. Finally, the supernatant was discarded, the pellet was air-dried for 10 to 15 minutes and resuspended in DEPC water.

The RNA was quantified using the NanoDrop spectrophotometer (Thermo Scientific NanoDrop™ 1000) and this measurement includes the absorbance of all molecules in the sample that absorb at the wavelength of interest. Since nucleotides absorb at 260 nm, and protein, phenol or other contaminants absorb strongly at or near 280 nm, the resultant 260:280 ratio will assure the purity of the sample. It is generally accepted that ratios of 1.8 for DNA and 2.0 for RNA, and the actual ratio will depend on the composition of the nucleic acid. RNA have a higher 260/280 ratio due to the higher ratio of Uracil compared to that of Thyminutese.[79]

Finally, RNA integrity was verified by running samples by electrophoresis in a 1% TAE-agarose gel with Ethidium bromide (0.1 %) and analyzing it in under UV light.

2.3.2 Removal of genomic DNA contamination

After RNA extraction, genomic DNA (gDNA) contamination is removed before cDNA synthesis and RT-PCR. To this end, samples were treated with DNase enzyme, from the DNA-free Kit (Ambion).

DNase treatment was performed using 10 µg of RNA to which 5 µl of DNase I 10x buffer, 1 µl of rDNase I (2U/ µl) and nuclease-free water, were added, to obtain 50 µl of reaction solution. The solution was homogenized gently and incubated at 37ºC for 30 minutes. After this, 5 µl of inactivation reagent were added to the mixture, vortexed for 1 minutes and incubated for 2 minutes at RT, mixing occasionally. The mixture was centrifuged for 1.5 minutes at 10000g (room temperature). At the end the supernatant containing the RNA was recovered.

The RNA was again quantified using the NanoDrop spectrophotometer (Thermo Scientific NanoDrop™ 1000).

2.3.3 Complementary DNA (cDNA) synthesis

Complementary DNA (cDNA) is synthetized from mRNA by the transcriptase reverse enzyme. Unlike gDNA it does not contain introns.

The synthesis of cDNA was carried out in a Thermal cycler (T100^{TM,} Bio-Rad) using 500 ng of DNase-treated RNA in which 1 µl of 10 µM deoxynucleotide-triphosphates (dNTPs), 1 µl of 100 mM random hexamers (short oligodeoxyribonucleotides of random sequences that anneal to random complementary sites on the target mRNA, to serve as primers for cDNA synthesis), 4 µl of 5x reaction buffer and DEPC water were added in a final volume of 19.3 µl. This mix was heated in the thermocycler to 65ºC for 5 minutes and then cooled at 4ºC for 5 minutes. Lastly 0.2 µl of Ribolock, RNase inhibitor (40 U/µl; Thermo Scientific), and 0.5 µl of RevertAid (200 U/µL; Thermo Scientific), reverse transcriptase, were added in a final volume of 20 µl. The samples were run in a synthesis reaction in the thermal cycler for 10 minutes at 25ºC, 60 minutes at 42ºC and 10 minutes at 70ºC. The cDNA was stored at -20ºC and dilutions in nuclease free water were prepared as needed.

2.3.4 Agarose gel DNA band purification

The purification of TAE-agarose gel is a way to recover DNA products for downstream applications including cloning and sequencing. In this study TAE-agarose gel DNA band purification was necessary for sequencing target DNA products amplified by RT-PCR (section 2.3.5.3) and by this way verify the primers specificity (section 2.3.5.1) and further prepare a standard curve (section 2.3.5.4) for every gene of interest.

The band purification was performed with GFX PCR DNA and Gel Band Purification Kit following the provided protocol. After the assembly of the band of interest, a capture buffer was added, mixed and stored at 60ºC for 30 minutes. After this, the obtained solution is putted through a column and centrifuged at 16000g for 30 sec. Then 500 µl of wash buffer was added to the column and centrifuged again at 16000g for 30 sec. At the end, DNA was collected by adding 20 µl of elution buffer in the column and centrifuged at 16000g for 1 minutes. The eluted DNA was -20ºC.

2.3.5 Polymerase chain reaction

PCR is a procedure where DNA is amplified *in vitro* with a three-step cycling process: denaturation, annealing and extension.

The first step is the thermal denaturation of a DNA sample by raising the temperature to 95ºC. The second step is the annealing, where primers, synthetic oligonucleotides, base pair with their complementary sequence in the DNA template. In this step, the temperature is slowly cooled to approximately 55ºC, (depending on the primers sequence). In the third step occurs the synthesis of the target DNA, which is mediated by the Taq DNA polymerase, an enzyme that resists to high temperatures and performs its catalytic function at approximately 72ºC. These three steps are repeated for a number of cycles and the amount of DNA duplicates at each cycle.

The PCR reactions were performed using for each sample 2 µl of 10X reaction buffer, 0.4 µl of dNTPs (10mM), 0.4 µl of each forward and reverse primers (10mM; Table 2), 0.08 µl of Taq DNA polymerase (5U/µl), 2 µl of diluted synthesized cDNA and milliQ water to reach a total 20 µl of reaction solution. PCR was carried out in a Thermal Cycler and began with a denaturation step at 95ºC for 5 minutes, followed by 22 cycles of denaturation at 95ºC for 30 sec, annealing at the respective temperature (Table 2) for 30 sec and synthesis at 72ºC for 30 sec. A final elongation step was performed at 72ºC for 5 minutes. At the end, the amplification was confirmed by running samples by electrophoresis in a 2% TAE-agarose gel with Ethidium bromide (0.1 %) and analyzing it in under UV light.

1. Primer design for target gene

The pair of primers used for PCR were the same used in qPCR. Although qPCR is a more sensitive technique requiring a smaller amplicon size for detection, a pair of primers design for it can be used in PCR, but not the other way around.

To design a specific pair of primers for each gene it is necessary to have a nucleotide sequence of the gene, against which the primers sequences will be homologous. This nucleotide sequence was obtained by searching the genome database of the National Centre for Biotechnology Information (http://www.ncbi.nlm.nih.gov/). The primers were designed using both Beacon Designer and Primer Premier Software taking in consideration general parameters such as:

- Primers size should be between 18 and 22 bp;
- Melting temperature should be between 52 and 58 ºC;
- Avoid runs of four or more bases, as it reduces annealing efficiency;

- Presence of G and C bases should be between 40 and 60%;
- Avoid the presence of secondary structures between the pair of primers such as hairpin, self-dimer and cross-dimer;
- Avoid cross-homology where a pair of primers can amplify a sequence in other gene, by running a BLAST (http://blast.ncbi.nlm.nih.gov/Blast.cgi) with the primers sequences.

Table 2 - Primer sequences for both PCR and RT-PCR reactions, forward (Fw) and reverse (Rv). The annealing temperature (Ta) at which the pair of primers anneal with complementary cDNA and the amplicon size in base pairs (bp).

Gene		Primer sequence (5' → 3')	Ta (ºC)	Amplicon size (bp)
PiT-1	Fw	CTGCTGTTACTGCTTCCGCTCCAC	60	163
	Rv	CAGGCTTGCTTCAGGGTCACTACAC		
PiT-2	Fw	AGAGGGTGGTGTGGAAATGAG	61	150
	Rv	CCGAAGCAGGCAGTGAGG		
NaPi2a	Fw	ACACGCCTGCCCATACG	61	156
	Rv	GCCCACTCCGACCATAGC		
NaPi2b	Fw	TTTGCTTGGCTGACTGGCTACC	60	140
	Rv	AGTGGATATGCCCTCTCAATGC		
α-klotho	Fw	GTAACCAGACCCAAGTGAACC	57	184
	Rv	GCAAACGCCAGAGCAGTG		
XPR1	Fw	GGGAACATCATTGCTACTGTCTTTG	60	181
	Rv	CCTGGTCCATCATCTGCTCAAG		
PCNA	Fw	GGTTGGTAGTTGTCGCTGTAGGC	60	130
	Rv	CTCAAACATGGTGGCGGAGT		
18S	Fw	TGACGGAAGGGCACCACCAG	60	158
	Rv	GCGTTCTTAGTTGGTGGAGCGATT		

2. 18S ribosomal (r) RNA PCR

To assess the quality and reliability of the synthesized cDNA, a PCR amplification of 18S ribosomal (18S) gene was performed, which served as an internal control, as it is expressed in abundance in all organisms and cell types. The PCR reaction was carried out as described in the section 2.3.5.

3. Real-Time qPCR

Real-Time quantitative PCR (qPCR) is a technique for gene-expression analysis very similar to traditional PCR. This method benefits from its sensitivity, large dynamic range as well as accurate quantification of specific gene expression that is measured after each round of amplification instead of the traditional PCR method. The concept of qPCR relies on the detection of amplified product using a fluorescent marker (SYBR Green) that binds to the DNA molecules. During amplification the fluorescent signal is increased, which is directly proportional to the amount of DNA produced during each PCR cycle.

This linear correlation between qPCR product and fluorescence intensity is used to calculate the amount of template present at the beginning of the reaction. The point where the fluorescence is first detected as statistically significant above the background is called the threshold cycle or Ct value.

The qPCR reactions were performed using, for each sample, 5 µl of Evagreen (Bio-Rad), 0.45 µl of each forward and reverse primers (10mM; Table 2), 2 µl of the diluted synthesized cDNA and milliQ water to obtain 10 µl of reaction solution. qPCR reactions were carried out in a StepOnePlus™ Real-Time PCR System (Thermo Scientific) and in an iCycler iQ™ Real-Time PCR Detection System (Bio-Rad), and began with a denaturation step at 95ºC for 30 sec, followed by 40 cycles of denaturation at 95ºC for 5 sec, annealing at the respective temperature (Table 2) for 10 seconds and synthesis at 60ºC for 10 sec. In the end, the amplification was confirmed by running samples by electrophoresis in a 2% TAE-agarose gel with Ethidium bromide (0.1 %) and analyzing it in under UV light.

4. Standard curve

A standard curve is obtained by running qPCR reactions of a dilution series of a template containing the fragment of interest. This standard curve can be used to relate the quantity of amplicon amplified from the known concentration of the starting material to a given Ct. To determine the starting amount of the target gene in the cDNA samples analyzed, their Ct obtained by qPCR is related to a concentration value obtained from the standard curve which is run in the same plate as the cDNAs.

5. Normalization

Normalizing to a reference gene is a simple method for internally controlling for error in qPCR, the amount of starting material and variation of reverse transcription efficiencies. Among the most used housekeeping genes is 18S rRNA, expressed constitutively and involved in basic housekeeping functions required for cell maintenance, and their expression is assumed to be unaffected by most experimental parameters.[80] Reference genes must be validated for a particular experimental condition and in this study were used 18S rRNA.

2.4 Statistical analyzes

The results are expressed as mean ± SEM. The difference between means for two groups and between means at different time-points within a single group was determined using Two-Way ANOVA multiple comparisons, explicitly Sidak's multiple comparisons test, where $p \leq 0.05$ was considered statistically significant.

3. Results and discussion

The first goal of this study was to evaluate gene expression of *PiT-1*, *PiT-2* and related genes in several tissues. With the resultant data, it aimed to better understand their distribution in tissues of the immune system, such as thymus and spleen, and tissues from the transport and absorption systems, such as kidney, duodenum, small intestine and bladder.

Later, to assess the role of extracellular phosphate, cotransporters *PiT-1* and *PiT-2*, and related genes in cell development and proliferation, the phosphate availability was modulated in cell culture assays. To this end, the EL-4 cell line was used, which is derived from a mouse thymic lymphoblastic lymphoma. These assays were complemented with assays performed with thymic cells from wild-type and leukemic transgenic mice, that developed acute lymphoblastic leukemia (ALL). Consequently, cell proliferation, ^{33}Pi uptake assays and gene expression associated with these assays were evaluated.

3.1 Gene expression in tissues

An initial examination of the expression pattern of phosphate cotransporters and associated genes was performed in a variety of tissues that belong to the renal and immune systems, among others. This had the purpose of better understanding and complementing the information already known from the literature.

The widespread expression of both *PiT-1* and *PiT*-2, described by Hernando et al attributing them a housekeeping role in phosphate transport[5,21], was confirmed in the quantitative real-time PCR analyses of RNA extracted from this tissues (Figure 3.1). The expression of both *PiT-1* and *PiT-2* was also detected in the small intestine and kidney justifying their moderate contribution (approximately 5%) to the transepithelial transport in these organs.[5] It was also observed a higher expression of *PiT-2* across tissues, when compared with *PiT-1*. The published information about *PiT-1* and *PiT-2* expression reveal a contrary information, where *PiT-1* is the more expressed in all tissues.[5] Although the functional distinction between these two proteins remains to be clarified, it is mentioned that both proteins share only 60% homology,[67] which may signify that both gene promotors only share 60% homology as well. As the need for two different proteins that are described to have the same function is not elucidated, this difference in their gene expression may be related with the possible difference that distinguish these two proteins and their possible need in different circumstances.

PiT-1 is associated with novel cellular metabolism roles like bone phosphate homeostasis[69], liver development[36], parathyroid function[34] and cell proliferation[66], and these different functions between these two proteins may require the synthesis of different quantities of mRNA.

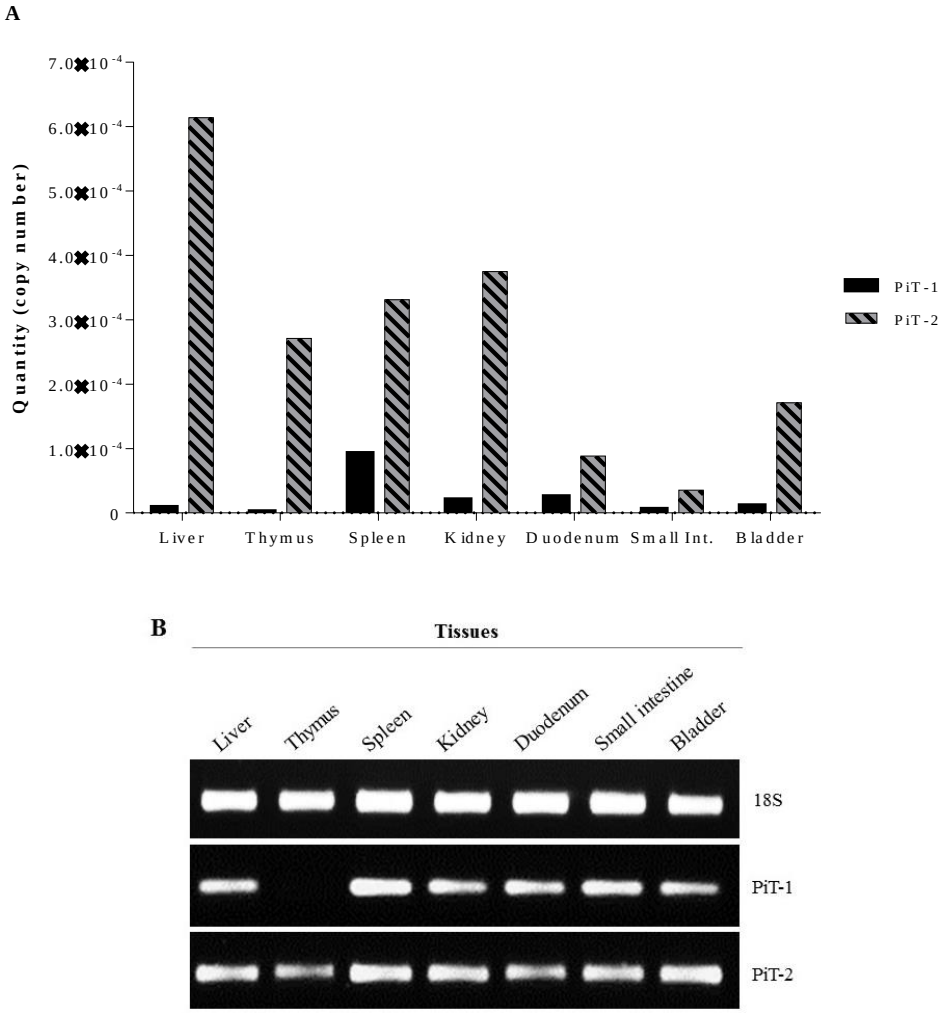

Figure 3.1 – Tissue-specific gene expression/distribution of type III Na^+/Pi cotransporters, *PiT-1* and *PiT-2*, in a wild-type strain mouse, C57BL/6. Both quantitative (A) and qualitative (B) expression were evaluated in tissues as liver, thymus, spleen, kidney, duodenum, small intestine and bladder. (A) Quantitative real-time PCR analyses of RNA from tissues was estimated in copy numbers where the results are represented in means (n=1; with 2 technical replicates). Data was normalized with the reference gene, 18S. (B) Qualitative gene expression was evaluated by running samples by electrophoresis in a 2% TAE-agarose gel with Ethidium bromide (0.1 %) and analyzing it in under UV light.

The main organs involved in phosphate homeostasis are the small intestine and kidney, and the main membrane transporters are NaPi-IIb and NaPi-IIa, respectively.[4,5,21] As depicted

in Figure 3.2, *NaPi-IIa* was mostly expressed in kidney with residual expression in the remaining organs, as described by Biber et al.[27,52,81] Its expression was 3-fold higher than the quantity of *PiT-1* and *PiT-2* (Figure 3.1), and *NaPi-IIb* (Figure 3.2). *NaPi-IIb* found to be mostly expressed in tissues of gastrointestinal tract such as duodenum and small intestine but also kidney, bladder and thymus, although its highest expression was detected in the small intestine as described by Fosters et al.[16,46]

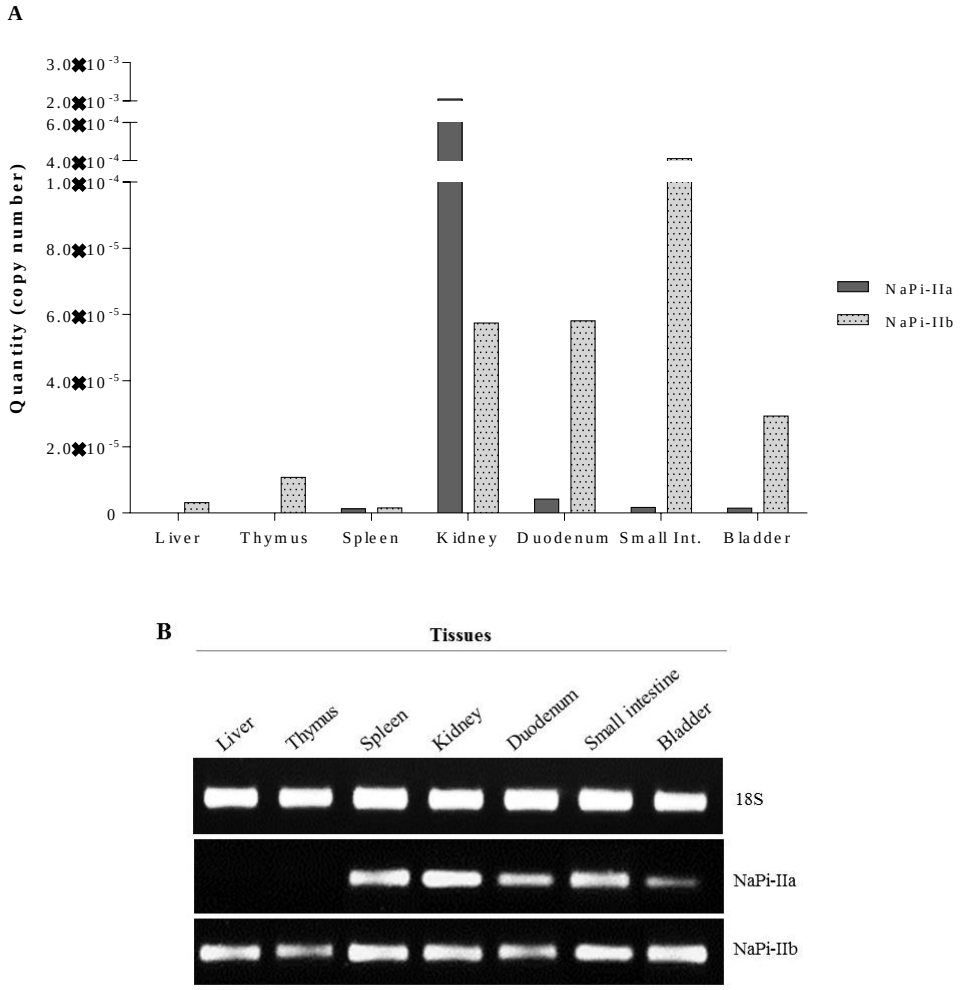

Figure 3.2 – Tissue-specific gene expression/distribution of type II Na^+/Pi cotransporters, *NaPi-IIa* and *NaPi-IIb*, in a wild-type strain mouse, C57BL/6. Both quantitative (A) and qualitative (B) expression were evaluated in tissues as liver, thymus, spleen, kidney, duodenum, small intestine and bladder. (A) Quantitative real-time PCR analyses of RNA from tissues was estimated in copy numbers where the results are represented in means (n=1; with 2 technical replicates). Data was normalized with the reference gene, 18S. (B) Qualitative gene expression was evaluated by running samples by electrophoresis in a 2% TAE-agarose gel with Ethidium bromide (0.1 %) and analyzing it in under UV light.

XPR1 had a broad expression pattern as described in the literature by Wege and Giovannini et al[6,38] although its highest expression was detected in the kidney and duodenum (Figure 3.3). This phosphate exporter is present in a range of cells such as pancreatic B cells, hepatocytes, jejunal enterocytes and renal proximal tubules cells[38], and the amount of cells transporting Pi is much higher when transporting in tissues. As seen in Figure 3.3, cells have different expression patterns among the tissues. In thymus, kidney and duodenum the number of copies was elevated, which for a housekeeping function a few are enough. This indicate that these tissues have an elevated rate of Pi export that would only be necessary if these same tissues had an elevated rate import, which is already known to be true. Body phosphate homeostasis is largely dependent by modulation of intestinal absorption of dietary phosphate, and renal phosphate reabsorption and excretion.[13]

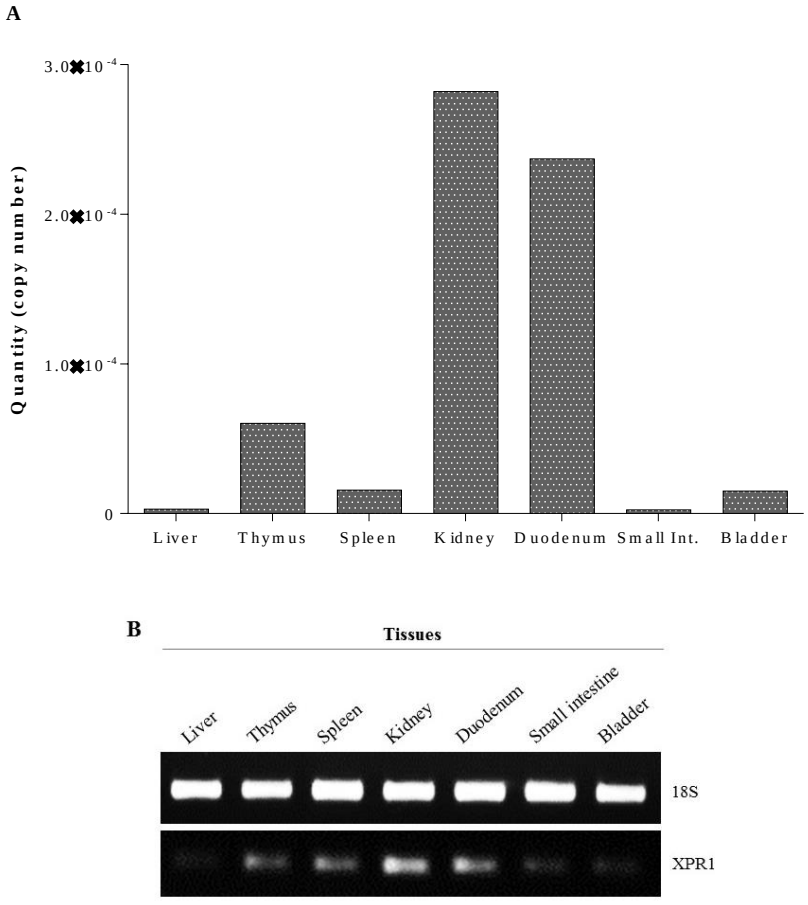

Figure 3.3 – Tissue-specific gene expression/distribution of a *XPR1*, a protein membrane appointed as a phosphate efflux transporter, in a wild-type strain mouse, C57BL/6. Both quantitative (A) and qualitative (B) expression were evaluated in tissues as liver, thymus, spleen, kidney, duodenum, small intestine and bladder. (A) Quantitative real-time PCR analyses of RNA from tissues was estimated in copy numbers where the results are represented in means (n=1; with 2 technical replicates). Data was normalized with the reference

gene, 18S. (B) Qualitative gene expression was evaluated by running samples by electrophoresis in a 2% TAE-agarose gel with Ethidium bromide (0.1 %) and analyzing it in under UV light.

The *α-klotho* is mainly expressed in renal distal tubules in kidney[59], which was verified in Figure 3.4 where it plays his major role as co-receptor of FGFR1. Although it was expressed in all analyzed tissues, its expression in kidney was 200-fold higher when compared to the other tissues. Again, expression in thymus was quite high, at the levels of what was observed in bladder, and much higher than that of the gastrointestinal tissues, an observation that requires further investigation.

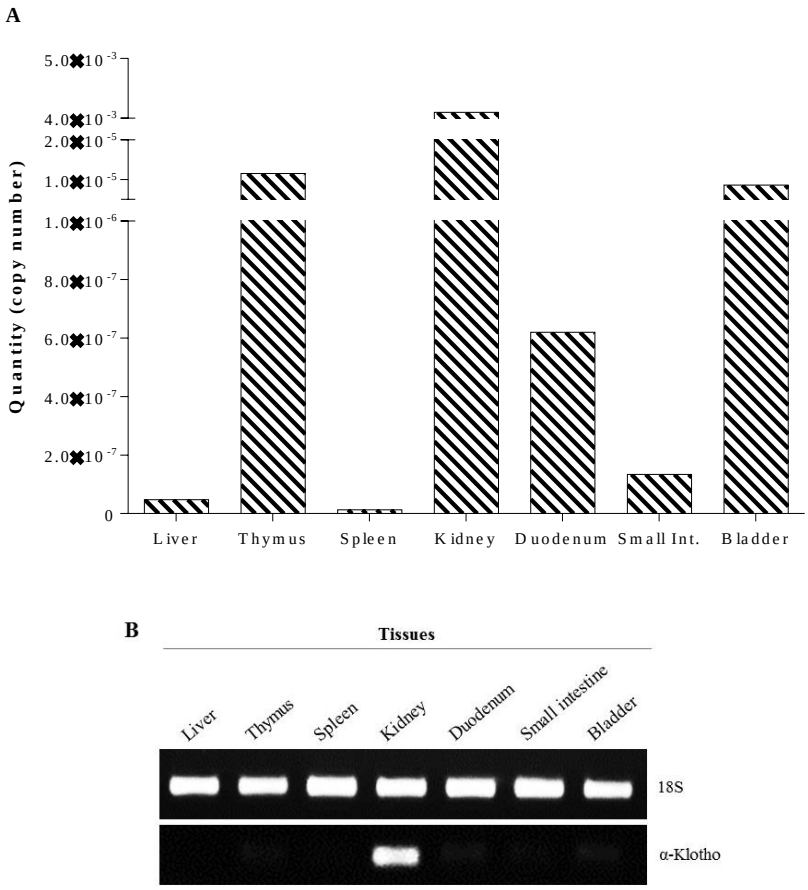

Figure 3.4 – Tissue-specific gene expression/distribution of *α-Klotho*, a FGF co-receptor, in a wild-type strain mouse, C57BL/6. Both quantitative (A) and qualitative (B) expression were evaluated in tissues as liver, thymus, spleen, kidney, duodenum, small intestine and bladder. (A) Quantitative real-time PCR analyses of RNA from tissues was estimated in copy numbers where the results are represented in means (n=1; with 2 technical replicates). Data was normalized with the reference gene, 18S. (B) Qualitative gene expression was evaluated by running samples by electrophoresis in a 2% TAE-agarose gel with Ethidium bromide (0.1 %) and analyzing it in under UV light.

3.2 EL-4 cells in FBS starvation and the recovery after a quiescent state.

To evaluate phosphate function and phosphate transporters expression and their role in cell proliferation, was used the EL-4 cell line. This line was previously established from a lymphoma from T cell. To better understand the cell line behavior in culture and cell proliferation pattern it was first performed a fetal bovine serum (FBS) starvation and followed by cell cycle reactivation after a quiescent stage.

An initial evaluation of the cell growth ratio (Figure 3.5) showed that after 48h of incubation with a low percentage of FBS (0.1%), cells entered in a stage of quiescence and inactivity. In the absence of growth factors, cells exit the cell cycle, termed G_0, characterized by low metabolic activity[82]. When comparing these two conditions, either normal or low serum, at the same time-point, 48h, it is evident that 0.1% FBS had a lower than 2-fold growth and the positive control (10% FBS) had almost a 7-fold growth. Upon the addition of FBS at 48h, quiescent and proliferative cell cultures were exposed to the same amount of FBS. It is evident in Figure 3.5 that 24h later, EL-4 cells rapidly recovered from the inactive into a proliferative state.[82]

Following the cell growth evaluation (Figure 3.5) a phosphate uptake assay was performed (Figure 3.6) to understand whether cell activity was associated with differential phosphate uptake. First, it was performed a phosphate uptake curve using a radioactive assay in normal conditions (10% of FBS and 6 mM phosphate) in EL-4 cells (Figure 3.6A and B) to estimate the rate of Pi uptake in EL-4 cells for future uptake assays. As it can be seen in Figure 3.6A, the rate of counts per minute (cpm's)/time of incubation counted in cells at the first 5 minutes was higher than 30 or 60 minutes later, where the number of cpm's did not even duplicate. In the first 5 minutes the number of cpm's had a rapid increase, velocity that when approaching the 15 minutes started to decrease and from 30 minutes on was reduced to almost stop, reaching a plateau phase, where the number of cpm's seemed to stagnate nearly below 1000. This indicates that at this point the tracer had nearly equilibrated with the Pi pool inside the cells.

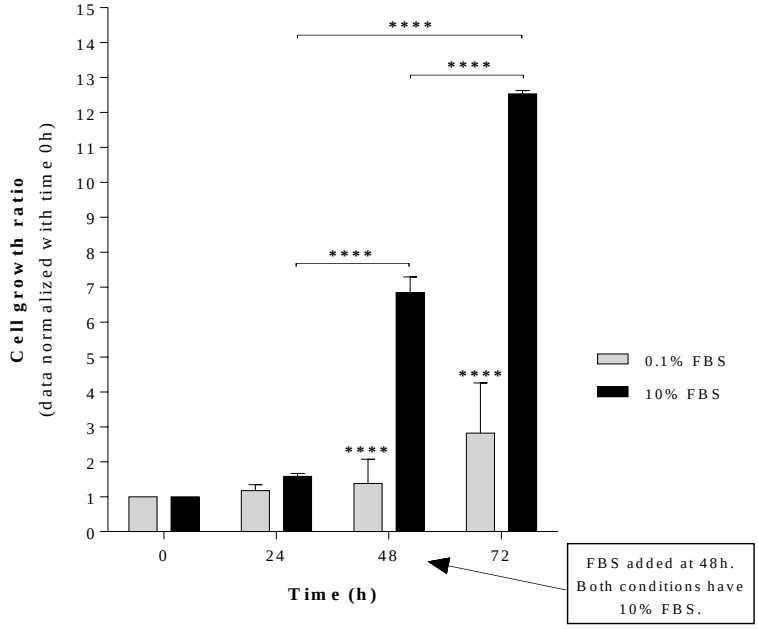

Figure 3.5 – Cell count in EL-4 cells in FBS starvation and the recovery after a quiescent state. Cells were seeded at a concentration of $2.5x10^5$ cells/ml in 100 mm Petri dishes at two different conditions: 0.1%FBS and control, 10%FBS. At the 48h time-point both cell culture medium was changed and replaced with medium with 10% FBS to evaluate cell recovery from a quiescent state. Cells were counted using Neubauer counting chamber at the indicated hours, and the results are shown as the mean ± SEM (n=3; with 3 technical replicates) of cell growth ratio were the data was normalized with the initial cell number (0h); ****, $p<0.0001$.

Figure 3.6B, shows the uptake of phosphate (nmol) per minute, data calculated using the number of cpm's (Figure 3.6A) and the exact quantity of Pi (nmol) present in the medium used (methodology section). At 5 minutes the uptake was about 3-fold higher than the rest of the time-points, and given the fact that the number of cells was always the same, this data suggests that the first minutes of cells incubation in the medium is the time where the highest uptake happens. At the beginning, the extracellular medium has a higher quantity of phosphate than intracellular, and the uptake occur rapidly until the cell starts to reach an equilibrium where the uptake of ions occurs at the same velocity as the exit of ions. This uptake course over time is prevalent in other cells as parathyroid gland cells[34] and intestinal brush border cells.[26]

Following these primary uptake tests, phosphate uptake assays were performed using two different FBS conditions, 0.1% and 10%, and only two different time-points, 5 and 30 minutes, corresponding where uptake occur rapidly and where the uptake reaches a plateau phase. At 48h there was a difference in uptake between the 0.1% and 10% FBS treatments, where in the first, the Pi uptake was lower than the positive control (Figure 3.6C). This data

would be expected when looking simultaneously to the cell growth data at the same conditions (Figure 3.5). Cells that entered a stage of inactivity because of the absence of growth factors have low metabolic activity, so will require less phosphate and then its uptake is also diminutesished.[82] It is also important to refer that the difference in the uptake between the two time-points (5 and 30 minutes) was maintained in both FBS conditions, although at 10% FBS this difference was sharper. At 72h, when cell recover to a proliferative stage, phosphate intracellular pool increases and so does increase the Pi uptake to content cellular needs. Here no significant differences were observed between the two treatments.

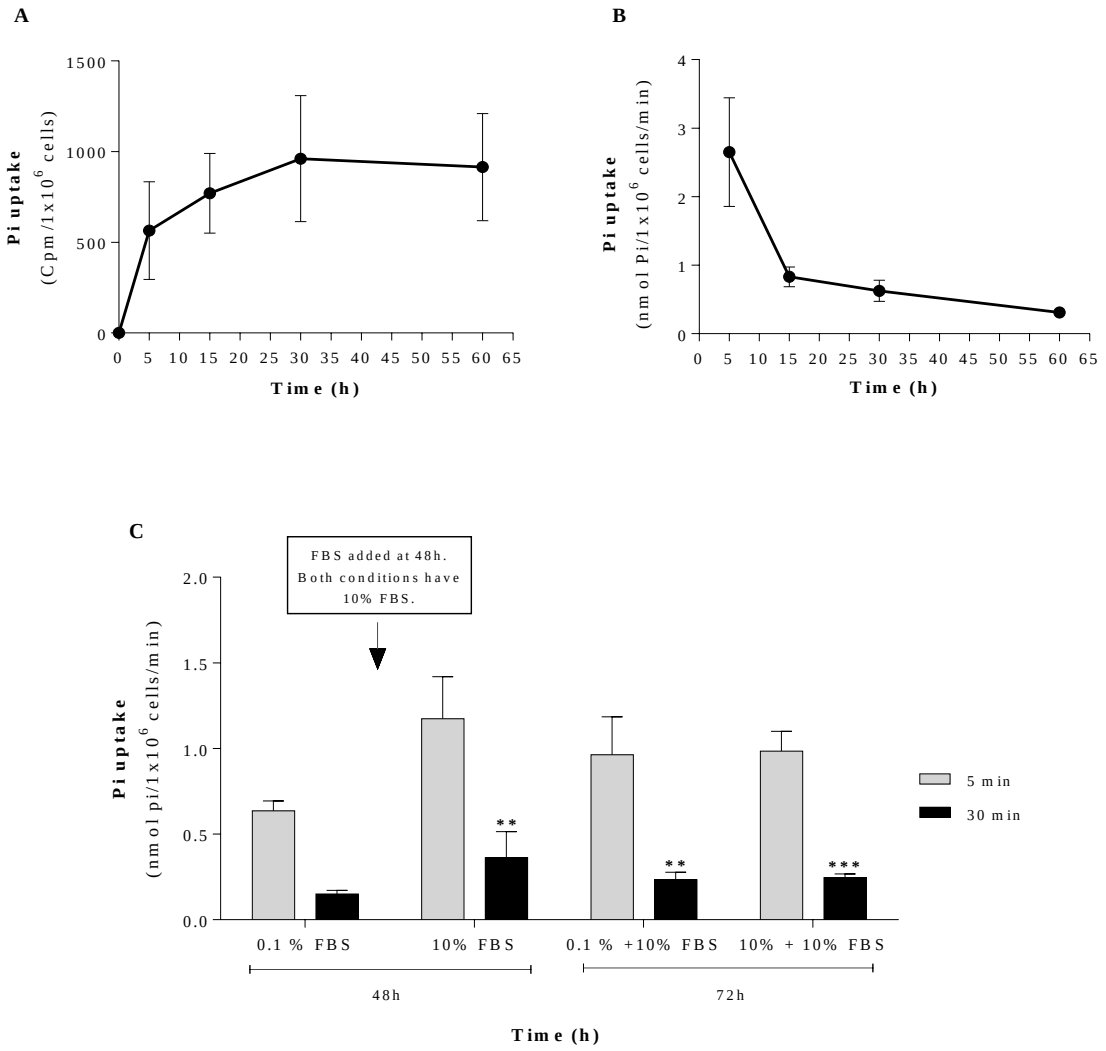

Figure 3.6 – Phosphate uptake in EL-4 cells in FBS starvation and the recovery after a quiescent state. Cells were seeded at a concentration of $2.5x10^5$ cells/ml in 100 mm Petri dishes at two different conditions: 0.1%FBS and control, 10%FBS. At the 48h time-point both cell culture medium was changed and replaced with medium with 10% FBS to evaluate cell recovery from a quiescent state. To calculate the Pi uptake over time it were collect 4 samples of $1x10^6$ cells for each time-point (0, 5, 15, 30 and 60 minutes) that cells were incubated with the ^{33}P radioisotope for the Pi uptake measurement. (A) The counts per minute (Cpm) measured by the

luminescence counter for each time-point are represented as mean ± SEM (n=2; with 4 technical replicates). (B) The phosphate uptake (nmol) per minute that enter the cell at each time-point is represented as mean ± SEM (n=2; with 4 technical replicates). (C) At the 48h time-point it were collect 4 samples of $1x10^6$ cells from each condition for each time-point (5 and 30 minutes) that the cells were incubated with the ^{33}P radioisotope. After that both cell culture medium was changed and replaced with medium with 10% FBS to evaluate cell recovery from a quiescent state. At the 72h time-point it were again collect 4 samples of $1x10^6$ cells from each condition to perform the same assay. The phosphate uptake (nmol) at each time-point is represented as mean ± SEM (n=2; with 4 technical replicates); **, $p<0.0026$; **, $p<0.0032$; ***, $p=0.0004$.

Later on, a quantification of gene expression was performed in EL-4 cells that had been submitted to the same FBS conditions (0.1% and 10%) at 48h and 72h. Although at 48h the cellular proliferation activity at 0.1% FBS was reduced, the gene expression of *PCNA* (Figure 3.7), a proliferating cell marker, did not seemed to show significant changes when compare with the positive control (10% FBS). It would be expected a lower *PCNA* expression when cell activity is reduced.[82]

It is also important to note that *α-klotho* expression in 0.1% FBS treatment was 2-fold higher than the proliferative stage (10% FBS). Secreted α-klotho functions as an aging suppressor. In certain cell lines, negates senescence phenotypes by regulating the mitogen-activated kinase pathway, an apoptotic pathway, and in mice, when overexpressed extends lifespan in about 20-30%. Also in mice, when disrupted, accelerates development of aging-like phenotypes.[57,58] In the 0.1% FBS treatment there is an absence of growth factors, so cells exit the cell cycle and there is no cell senescence. It makes sense that *α-klotho* expression was higher, to maintain this no-aging state.

Adding to this data, both *PiT-2* and *XPR1* decreased in the quiescent stage, more significantly *XPR1* that showed a 9-fold lower expression than at proliferative stage. This data may suggest that in a stage of low cell proliferation both phosphate import, partially executed by *PiT-2*[4,5], and export, possibly performed by *XPR1*[38], in cells are reduced corresponding to cell necessities.

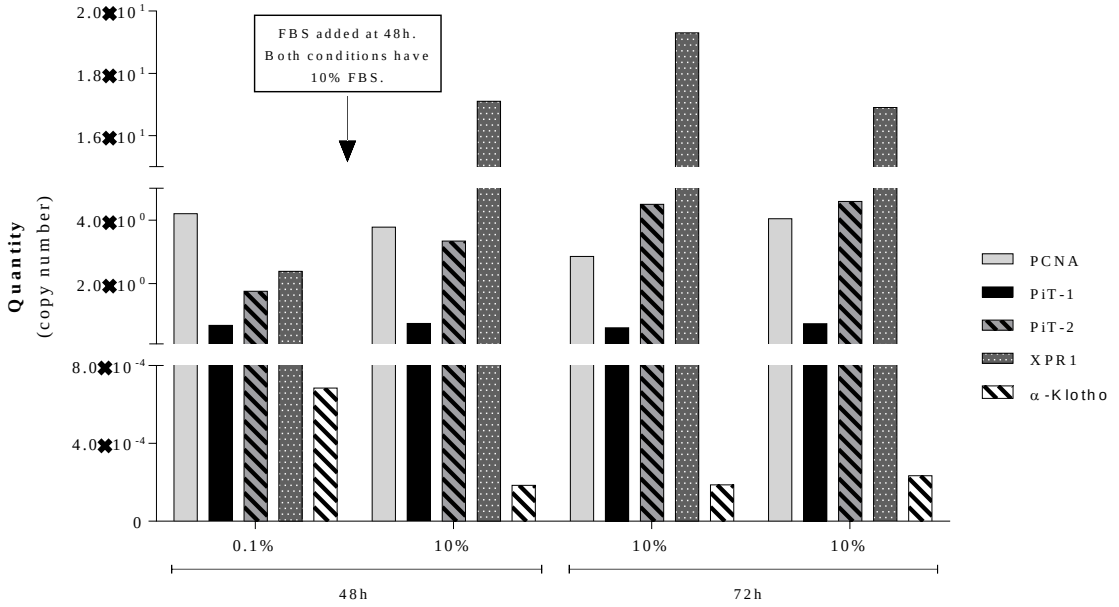

Figure 3.7 – Gene expression in EL-4 cells in FBS starvation and the recovery after a quiescent state. For the gene expression was recovered from each indicated time-point (at 48h before the addition of FBS and at 72h) $9x10^6$ of cells, $1x10^6$ cell for each technical replicate in each experimental replicate, that were combined in a single sample. The quantitative expression of *PCNA*, a proliferating cell marker, *PiT-1* and *PiT-2*, type III Na^+/Pi cotransporters, *XPR1*, phosphate efflux transporter and *α-klotho*, FGF co-receptor, was evaluated by real-time PCR analyses where the RNA from cells was estimated in copy numbers and the results are represented in means (n=1; with 1 technical replicate). Data was normalized with the reference gene, 18S.

3.3 EL-4 cells proliferation under variable phosphate availability

Following the FBS starvation experiment, a phosphate availability assay was performed in EL-4 cells for a period of 96h. Five different concentrations of phosphate were tested and in all these conditions phosphate free medium (with residual phosphate of 0.32 mM), was used, to which different amounts of phosphate (phosphate Sorensen buffer; annex 1) were added as described in the methodology section. The most obvious phosphate concentration to be tested was 6 mM since it is the one used as standard in cell cultures, as in the positive control. Then was decided to cover a range of 4 concentrations from nominal 0 mM (0.32 mM – residual Pi concentration) until an highly excessive amount (18 mM Pi) and including 3 mM concentration that is similar to the concentration in the extracellular plasma, although only the ionic form, corresponding to 1.5 mM, is immediately available to cells.[12,13,44]

Looking at the cell growth ratio (Figure 3.8A) is evident that at every 24h the cells of positive control (6 mM) duplicate, evidence that is followed by the 6 mM Pi condition. In the remaining Pi concentrations tested, the cells followed the 2-fold growth of the positive control

up to 48 h, from which it becamed evident a stagnation in the cell growth. The slower cell growth above the 48h of culture it is most likely to not be due to cell medium saturation, given the fact that all conditions had the same cell culture incubation (96h) and the positive control (6 mM) and the equivalent 6 mM, where the phosphate buffer was added to culture medium, followed the expected path. It may be related with pH variation upon addition of the phosphate buffer in the medium. This data demonstrates that the Pi concentration at what cells keep their optimum function does not differ much since 3 mM below or above was enough to retain cell proliferation above 48h of culture. Although one would expect optimal conditions between 1.5 and 3 mM, but cells seem to remain better at 6 mM. The possible explanation to this result would be the fact that these cells are maintained at 6 mM in a standard culture for so long prior to these treatments that when changing conditions, for both or less phosphate, cells sense these variations as unusual and their proliferation is reduced. Interestingly, many cultivated cells perform better at elevated phosphate conditions. In a specific case, Pombinho et al showed that fish bone-derived cells required above normal physiological conditions to multiply and additional phosphate to mineralize, with 11.8 and 10.9 mM phosphate in L-15 and D-MEM culture medium, respectively, but only upon the addition of high values of calcium (final free calcium concentrations of 5.3 and 5.8 mM, about 4 times the ionic values in vertebrate plasma) would initiate mineralization of the cellular matrix.[83] The added value of this high phosphate is intriguing but it may be related to apparent dependence of the internal medium of external phosphate concentrations demonstrated in the uptake assays (Figure 3.9).

Alongside with the cell growth measurement it was also performed a cell viability assay, using the MTT (methodology section). It is apparent that when comparing the 48h with the 96h time-point, there was a general decrease in cell activity in the first one (Figure 3.8B). In this viability assay, cell proliferation differences shown in the various phosphate conditions in the cell growth ratio (Figure 3.8A) are not that evident, but one thing is clear, longer the duration of the assay, lower the cell proliferation.

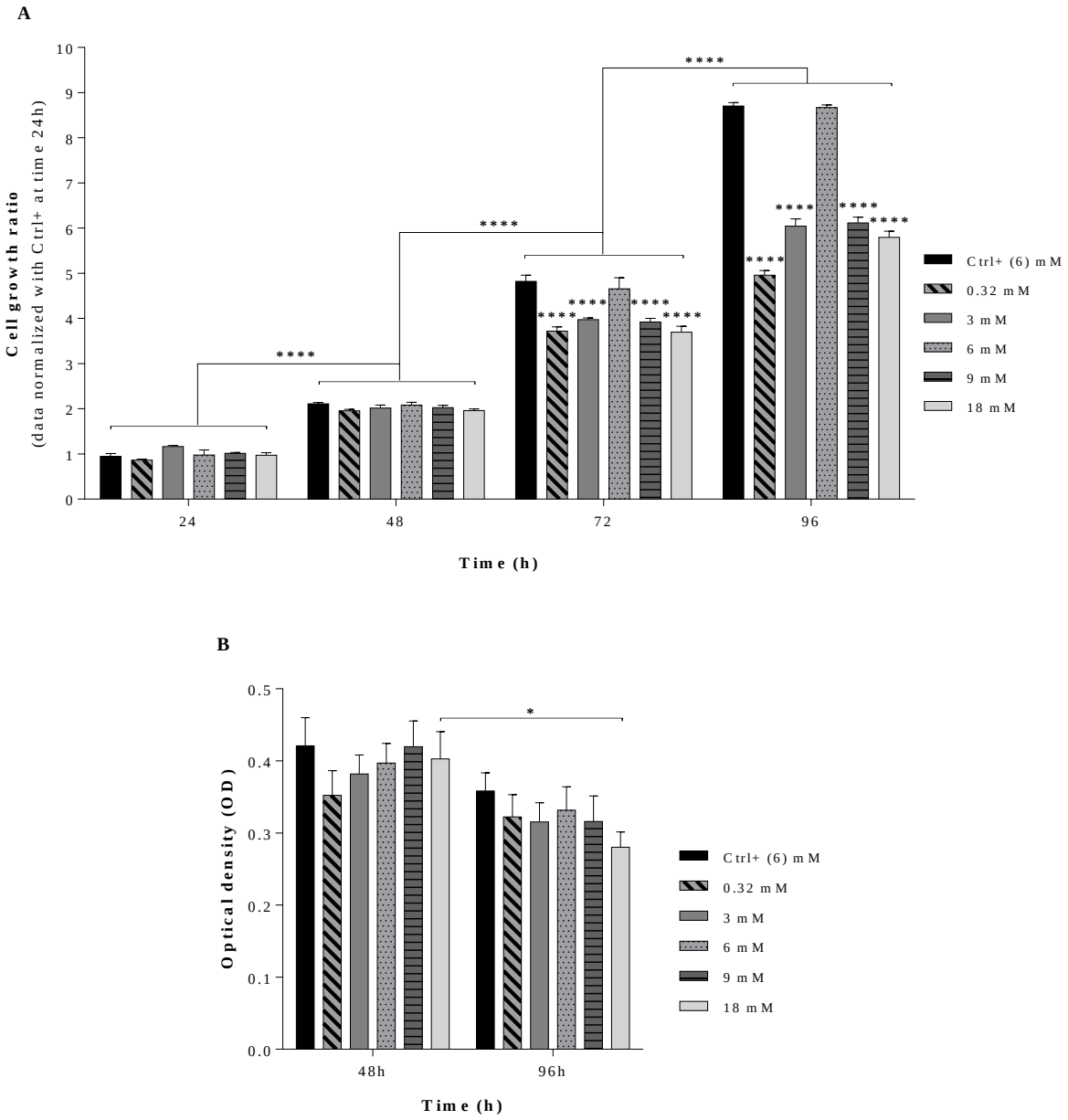

Figure 3.8 – Cell count and viability in EL-4 cells under variable phosphate availability. (A) Cells were seeded at a concentration of $2.5x10^5$ cells/ml in 24 well plate in the different phosphate concentrations indicated (0.32, 3, 6, 9 and 18 mM) using as positive control 6 mM. Cells were counted using Neubauer counting chamber at the indicated hours, and the results are shown as the mean ± SEM (n=5; with 3 technical replicates) of cell growth ratio were the data was normalized with the initial cell number (24h); ****, $p<0.0001$. (B) Cells were seeded at a concentration of $2.5x10^5$ cells/ml in 96 well plate in the different phosphate concentrations indicated (0.32, 3, 6, 9 and 18 mM) using as positive control 6 mM. At the indicated hours, the MTT assay was performed, the absorbance was measured on an ELISA plate reader at a wavelength of 570 nm and the results are presented as mean ± SEM (n=3; with 3 technical replicates); *, p=0.0410.

Phosphate uptake was carried out in EL-4 cells under altered Pi concentrations previously described (Figure 3.8A and B). In continuity with the primary uptake tests performed (Figure 3.6A and B) only two different time-points, 5 and 30 minutes, were used.

In the Figure 3.9 it is shown the phosphate uptake in EL-4 cells after an incubation of 96h with various Pi concentrations in the cell culture medium. Is evident that the higher the Pi concentration present in the cell culture medium, the higher the uptake. This perception becomes more evident at the 5 minutes time-point of incubation with the ^{33}Pi radioisotope, rather than at the 30 minutes time-point, confirming the Figure 3.6A and B data and the reason why this two time-point were chosen. It is possible that a sensing mechanism allowed the cell to adjust to such Pi variations at long-term.[17,62] Although at higher Pi concentrations (9 and 18 mM) the difference between the two time-points became more significant, if only taken in account the 30 minutes growth along the Pi conditions. It is evident that besides the existence or not of a sensing mechanism, cellular uptake depends on the Pi quantity present in the extracellular medium, which points to a less than perfect modulation of Pi balance. This deserves further investigation.

When comparing the positive control (6 mM) with the Pi condition where the same amount was added to the medium and even at lower concentrations (3 mM), there seems to be a slight rise in these last ones, although this increment was not significant.

At the 48h and 96h time-point of the cell culture was assessed a gene expression quantification (Figure 3.10) of the type III Na^+/Pi cotransporters, *PiT-1* and *PiT-2* (Figure 3.10A and B), type II Na^+/Pi cotransporters, *NaPi-IIa* and *NaPi-IIb* (Figure 3.10C and D), phosphate efflux transporter, *XPR1* (Figure 3.10E), proliferating cell marker, *PCNA* (Figure 3.10F) and FGF co-receptor and anti-aging gene, *α-klotho* (Figure 3.10G). These results came from primary tests which need to be repeated and confirmed but it is showed that the majority of the genes had lower expression at 96h comparing with 48h in any phosphate concentration, which can be associated with a lower cell viability at 96h (Figure 3.8B). This lower cell metabolic activity will be reflected in the reduced mRNA transcription and consequent protein transduction. Supporting this hypothesis is the *PCNA* expression (Figure 3.10F), a proliferating cell marker, that at 96h was expressively lower compared with 48h, being also the only gene where this difference was most noticed.

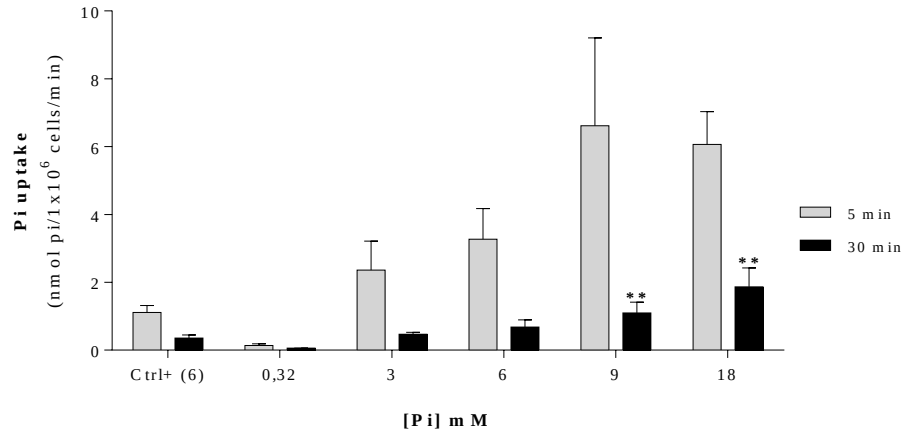

Figure 3.9 – Phosphate uptake in EL-4 cells under variable phosphate availability. Cells were seeded at a concentration of $2.5x10^5$ cells/ml in 24 well plate for a total of 96 h in the different phosphate concentrations indicated (0.32, 3, 6, 9 and 18 mM) using as positive control 6 mM. To calculate the Pi uptake in cells after an incubation of 96 h, it were collect 4 samples of $1x10^6$ cells from each condition for each time-point (5 and 30 minutes) that the cells were incubated with the ^{33}P radioisotope. The phosphate uptake (nmol) at each time-point is represented as mean ± SEM (n=2; with 4 technical replicates); *, p=0.0132; **, 0.0023<p<0.0051; ***, 0.0002<p<0.0006; ****, p<0.0001.

Looking at the cotransporters *NaPi-IIa* and *NaPi-IIb* (Figure 3.10C and D), there seemed to be no pattern change according to phosphate variation or in the different time-points (48h and 96h). For example, the expression quantity at 0.32 mM Pi was lower compared with 18 mM Pi, a much higher concentration, but higher than 6 mM Pi. The EL-4 cell line used in these experiments derive from a T cell lineage and as described previously, *NaPi-IIa* and *NaPi-IIb* execute their function mainly in kidney and small intestine, respectively, although their expression has been detected in other tissues (Figure 3.2). *NaPi-IIa* and *NaPi-IIb* showed a lower expression comparing with both *PiT-1* and *PiT-2*, in a fold range between 3 and 4, being *NaPi-IIa* the gene that was less expressed. This difference between both SLC families had already been seen in Figure 3.1 and 3.2 and it was in concordance with data published by Biber et al, where both *PiT-1* and *PiT-2* have an expression 100-fold range higher than *NaPi-IIa* and *NaPi-IIb*.[5]

When it comes to the cotransporters *PiT-1* and *PiT-2* (Figure 3.10A and B), there seems to be a slight decrease in their expression at 96h time-point, but there was no pattern change according to phosphate variation. There was also no consistence between the positive control (6 mM) and the equivalent Pi added condition. If the uptake increases with higher extracellular phosphate, the transporters that are responsible for that uptake should also increase, specially PiT-1 and PiT-2 that play their function in all types tissues.[31] It was notable a 10-fold higher expression of *PiT-2* comparing with *PiT-1*, a difference that was also seen in Figure 3.1, 3.2,

3.3, 3.4 and 3.7, however in a different fold range. A potential role of PiT proteins in Pi sensing has been described as being important for cellular functions, such as proliferation[17,66], and although there are indications of an existent sensing mechanism (Figure 3.9), nothing in the Figure 3.10A and B points to that case.

Several studies have suggested that PiT-1 may be involved in the p38 mitogen activated protein kinase (MAPK) and tumor necrosis factor alpha (TNFα) apoptotic pathways[35,66] The p38 MAPK pathway regulates cellular functions such as gene expression, differentiation, mitosis, cell survival and proliferation, but is described to have a key role in delaying the G2/M phase transition.[84] Here it was observed that *PiT-1* expression was downregulated at all phosphate concentrations at 96h which is when cell viability was also reduced according to the MTT assay. However it was not analyzed the frequency of cells in each phase of the cellular cycle nor used any marker for cellular apoptosis. Beck et al showed that *PiT-1* depletion enhanced the phosphorylation of p38 MAP kinase thus affecting cytokinesis in HeLa cells, in parallel with a reduction of tumor growth in nude mice inoculated with *PiT-1* knockdown HeLa cells.[35] TNFα is a cytokine that may activate either anti-apoptotic or pro-apoptotic pathways[85] and apparently also increase the expression of PiT-1 in diverse cell types[86]. *PiT-1* depletion increases the TNFα pro-apoptotic activity mediated by the caspase-8 pathway.[66]

The effect of *PiT-1* in cell proliferation and protection against apoptosis was not shared with PiT-2.[35,66] However, in assays performed in this investigation, both genes show similar apparent reduction in expression at 96h when compared to 48h, which occur in parallel with a decrease in the expression of the proliferative marker gene *PCNA.* So both PiT-1 and PiT-2 appear to be important for EL-4 proliferation, although their specific role was not investigated.

This TNFα-induced up-regulation of *PiT-1* prompted the question whether *PiT-1* could be involved in protection against apoptosis. Later it was discovered that PiT-1 depletion increases the TNFα pro-apoptotic activity mediated by the caspase-8 pathway.[66] In both proliferation and protection against apoptosis it was shown that the effect of PiT-1 was not shared with PiT-2.[35,66]

In Figure 3.10E and G is shown that both *XPR1* and *α-klotho* expression pattern are unclear, as the other previous genes according to phosphate variation or in the different time-points (48h and 96h), although XPR1 seemed to be highly expressed in the highest phosphate concentration, perhaps to facilitate Pi excretion from the cell. *PiT-1* had the same expression range of *XPR1*, or even higher, as is the case of *PiT-2*. Phosphate uptake performed by these

two cotransporters in these cells during this assay had as response, the Pi export by XPR1[38] to maintain the intracellular pool equilibrium. This *XPR1* high expression was due to a response to cellular needs.

In conclusion, the growth rate variances caused by the different Pi availability in the cell culture medium, the increase in the uptake along with extracellular Pi increase, and gene expression indicate that both PiT-1 and PiT-2 appear to be important for EL-4 proliferation.

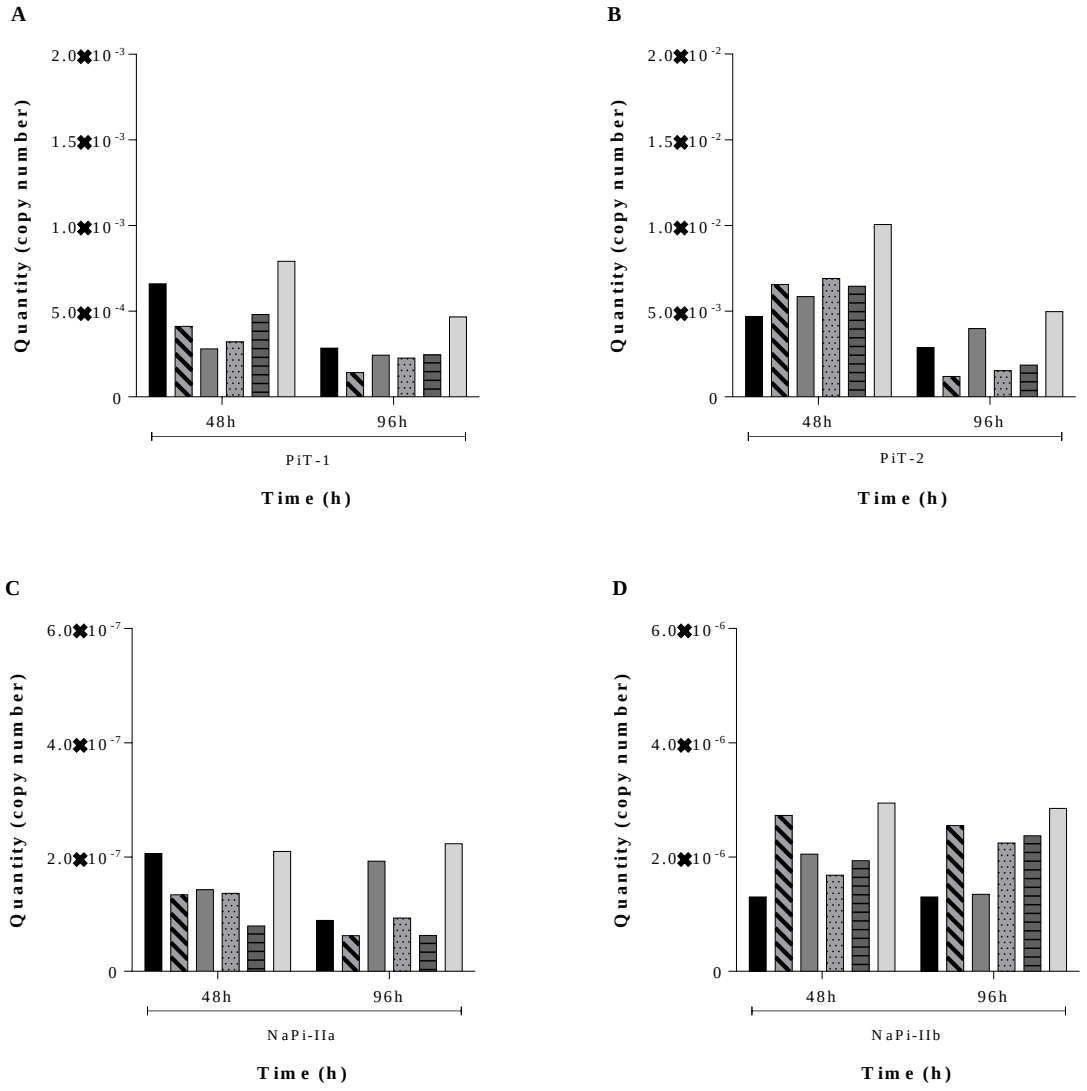

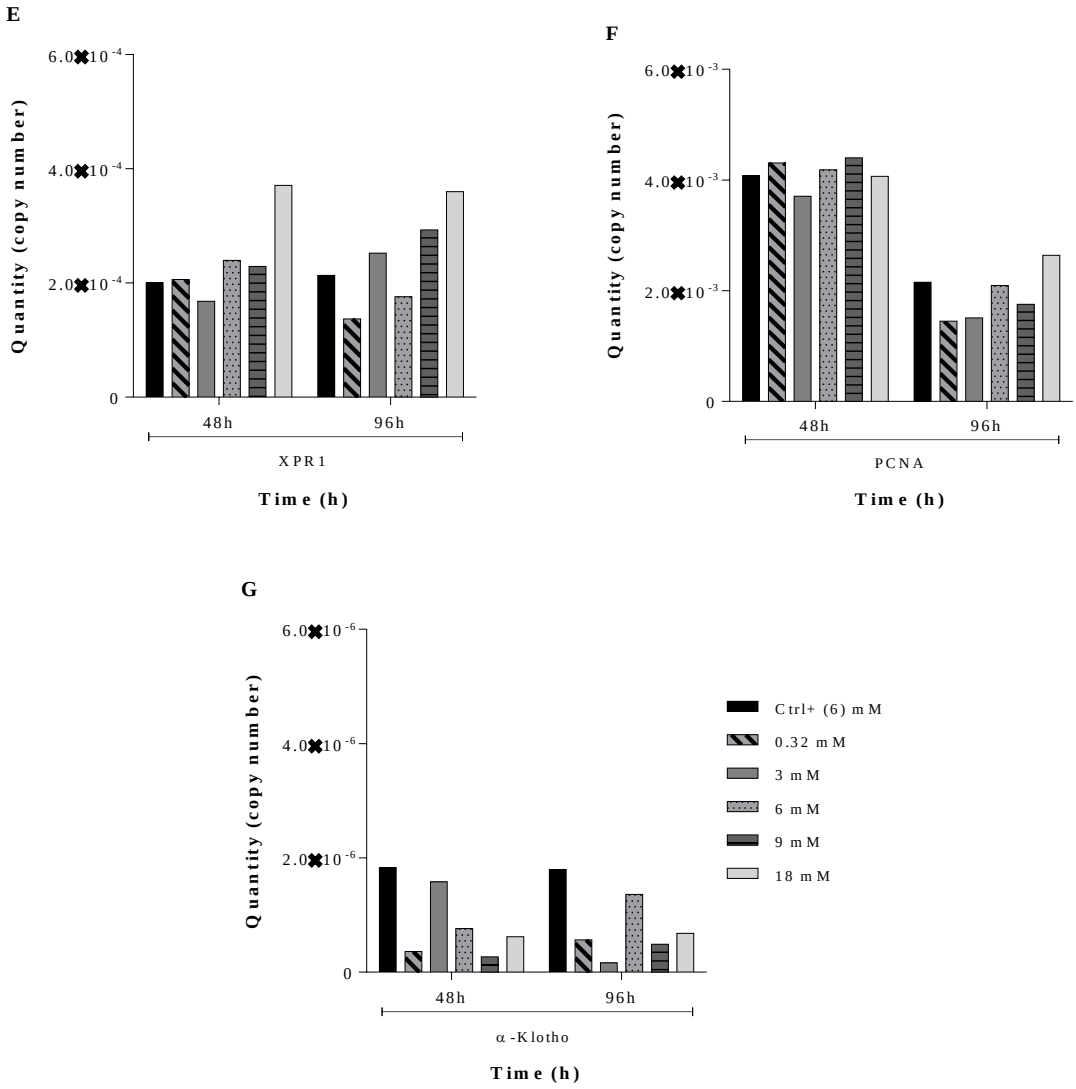

Figure 3.10 – Gene expression in EL-4 cells under variable phosphate availability. Cells were seeded at a concentration of 2,5x10^5 cells/ml in 24 well plate in the different phosphate concentrations indicated (0.32, 3, 6, 9 and 18 mM) using as positive control 6 mM. For the gene expression was recovered from each indicated time-point 9x10^6 of cells, 1x10^6 cell for each technical replicate in each experimental replicate, that were combined in a single sample. Quantitative expression of (A) *PiT-1* and (B) *PiT-2*, type III Na^+/Pi cotransporters, (C) *NaPi-IIa* and (D) *NaPi-IIb*, type II Na^+/Pi cotransporters, (E) *XPR1*, phosphate efflux transporter, (F) *PCNA*, proliferating cell marker and (G) *α-klotho*, FGF co-receptor and anti-aging gene, was evaluated by real-time PCR analyses where the RNA from cells was estimated in copy numbers and the results are represented in means (n=1; with 1 technical replicate). Data was normalized with the reference gene, 18S.

3.4 Wild-type and leukemic thymic cells from mice

Both lymphoblastic lymphoma and leukemia derive from the same cell type, lymphocytes. The EL-4 cells are an established cell line and the leukemic cells collected from mice are not established, which means that although it were prevenient from a TEL-JAK2

transgenic mice, there was no way to be certain if all the collected cells were leukemic cells, with the possibility of being present some wild-type cells. So these two cell types and the assays that have been performed in both of them complement each other. As control it were used cells from wild-type animals as well.

A preliminary cell count was performed for an initial distinction in cells from the different types of animals. Tumorigenic tissues are characteristic for resisting to cell death, enabling replicative immortality and an enhanced proliferative rate that will result in abnormal cell growth higher cell number.[75] This last characteristic were observed in Figure 3.11 where the number of cell present in leukemic thymus is 2-fold higher than the cells in wild-type thymus.

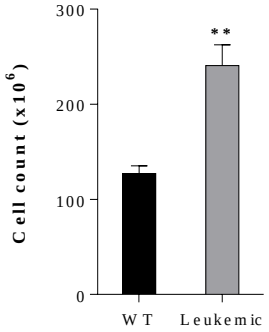

Figure 3.11 – Cell counts in the WT and leukemic thymus. Thymus was recovered from mice and cell extraction was performed right after. Cells were counted using Neubauer counting chamber at the indicated hours, and the results are shown as the mean ± SEM (n=3) of cell number present in thymus from each type of animal; **, p=0.0011.

After recovering cells from thymus and to guarantee that the mice was actually leukemic as exterior evidences indicated (slower locomotion movements, overweight and swelling of the thymus, spleen and lymph nodes showed) an immunostaining technique was used. The results represented in Figure 3.12 show existence of two different cell types, each one in a different animal. Mature wild-type thymus cells, before exiting the thymus, express both CD4 and CD8 (double positive) and represent the bigger percentage of cells.[72,73] In Figure 3.12A, double positive cells represent about 81%, comparing with single positive and double negative cells, represented in a much lower percentage.

In leukemic mice, the mature leukemic cells express a higher quantity of CD8 when comparing with wild-type cells, which will result in a percentage of single positive CD8 equal or even bigger to the double positive cells.[72,73] And in Figure 3.12B the percentage of double positive cells is 30.11% and the CD8 single positive is higher, 42.84%, showing that they were in fact leukemic cells recovered from an diseased animal.

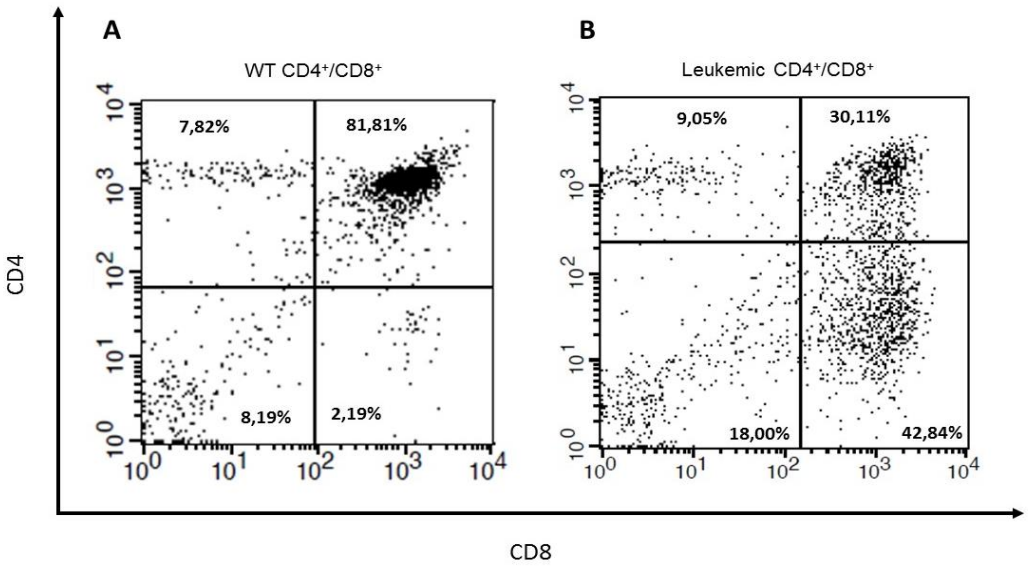

Figure 3.12 – Cell surface fluorescent immunostaining in wild-type and leukemic thymus cells from mice, C57BL/6 strain and TEL-JAK2 transgenic, respectively. Cell suspensions from thymus were obtained from wild-type and transgenic leukemic animals. The CD4 and CD8 expression pattern of unsorted cells from (A) wild-type and (B) leukemic animals was determined by flow cytometry. For each experiment, 1x106cells were incubated with anti-CD4-PE (Y-axis) and anti-CD8-PE/Cy5 (X-axis) and analyzed by flow cytometry. The results were computed from the acquisition of 10 000 events. The relative percentage of each subpopulation is indicated in the corresponding area of the diagrams.

Later on, after confirming that the collected cells from thymus where actually from different animals, WT and leukemic, a gene expression was assessed to quantify and evaluate the differences between the two different cell types. In general, gene expression in this thymic collected cells had a lower quantity when comparing with the same gene expression in EL-4 cells assays.

PCNA, a proliferative marker, has a lower quantity expression in leukemic cells comparing with wild-type cells. This outcome was unexpected, given the fact that tumorigenic cells are characterized for a sustaining proliferative signaling as well as enabled replicative immortality.[75]

PiT-1 had lately been associated with cell proliferation and cell density. Depletion of *PiT-1* expression in HeLa cells resulted in reduced cell proliferation and impaired mitosis,[35] and over-expression of *PiT-1* increased proliferation in density-inhibited cell lines.[70] In the Fi. 3.13, this was not observed, as the expression of *PiT-1* in leukemic cells was actually lower comparing with wild-type cells. *PiT-2* had also the same expression, where its expression in WT cells was higher than in leukemic cells. It is also noteworthy the expression pattern between *PiT-1* and *PiT-2*, where *PiT-2* was about 2-fold higher than *PiT-1* in both WT and leukemic cells, data also seen in Figure 3.7 and 3.10.

Relatively to *NaPi-IIa* and *NaPi-IIb*, both of them are more expressed in leukemic cells than WT cells and it is also important to notice that they both have a 300-fold lower expression when comparing with *PiT-1* and *PiT-2*, results also observed in Figure 3.1A, 3.2A and 3.10, and described by Biber et al.[5]

XPR1 (Figure 3.12C) did not show any differences between WT and leukemic cells, although both *PiT-1* and *PiT-2* had expressed those differences. Comparing both Pi importers and exporter, *XPR1* had a much lower expression. Phosphate uptake performed by *PiT-1* and *PiT-2* did not had an adequate response by XPR1.[38] Somehow in this case the exporter housekeeping role is maintained at a low rate due to cellular needs.

α-klotho showed a 2-fold higher expression when comparing the leukemic with WT cells (Figure 3.12E). Novel studies have been relating α-klotho as a tumor suppressor by inhibiting Wnt signaling pathway, well known for its role in cell fate, proliferation and migration.[59] Given this, it would be expected a higher expression of *α-klotho* in wild-type cells, where tumor suppression is being placed, but this was not observed, as it happened the contrary.

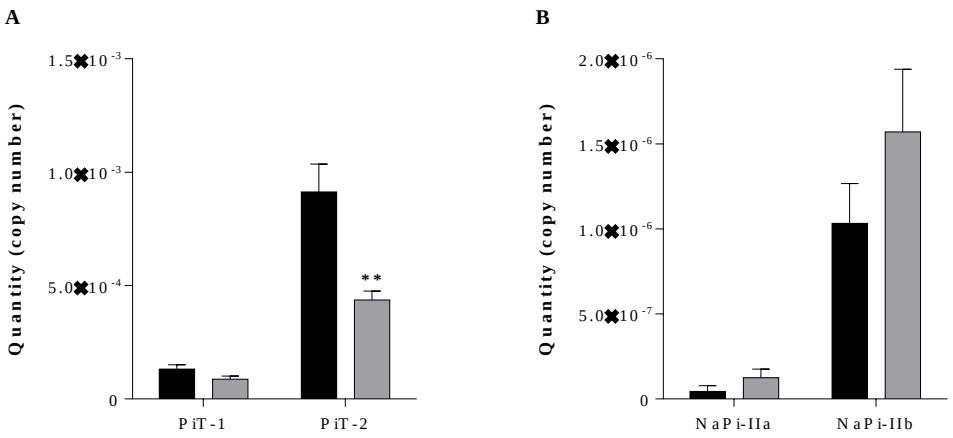

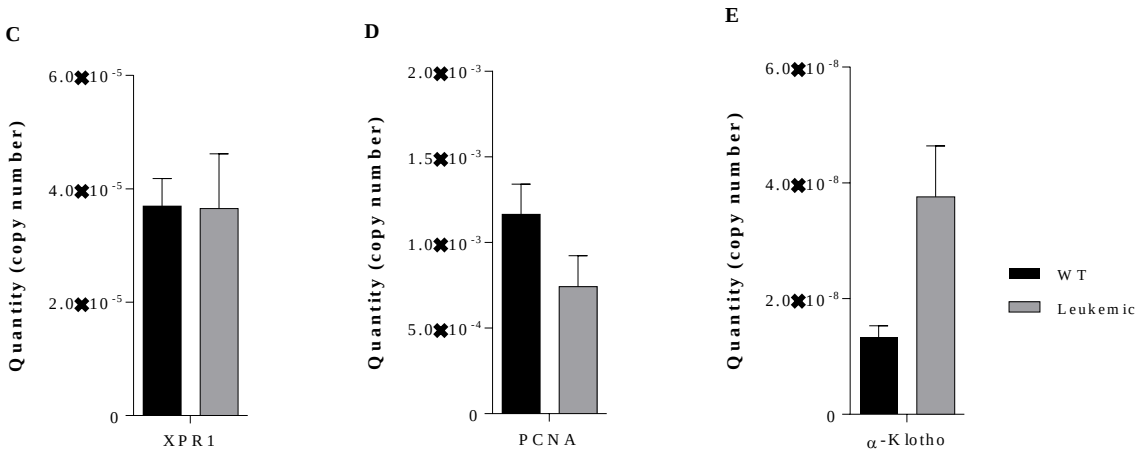

Figure 3.13 – Gene expression in in wild-type and leukemic thymus cells from mice, C57BL/6 strain and TEL-JAK2 transgenic, respectively. It were recovered thymus cells from each animal type, wild-type (WT) and leukemic. For the gene expression were used $30x10^6$ cells, $10x10^6$ cells for each animal that were combined in a single sample. Quantitative expression of (A) *PiT-1* and *PiT-2*, type III Na^+/Pi cotransporters, (B) *NaPi-IIa* and *NaPi-IIb*, type II Na^+/Pi cotransporters, (C) *XPR1*, phosphate efflux transporter, (D) *PCNA*, a proliferating cell marker and (E) *α-klotho*, FGF co-receptor, was evaluated by real-time PCR analyses where the RNA from cells was estimated in copy numbers and the results are represented in means ± SEM (n=3; with 2 technical replicate); **, p=0.0018;. Data was normalized with the reference gene, 18S.

3.5 Wild-type and leukemic thymic cells under variable phosphate availability

A phosphate uptake assay was performed in cells *ex vivo*, similar to what was described for EL-4 cells. A phosphate uptake curve using a radioactive assay in WT cells in normal conditions (10% of FBS and 6 mM phosphate) was carried out to estimate the velocity of the Pi uptake and verify if the response was as for EL-4 cells.

As it can be observed in Figure 3.14A, the number of cpm's counted in cells at the first 5 minutes was higher when comparing with the next time-points. From the 15 minutes on the number starts to decrease reaching around the same number over time. In Figure 3.14B is showed the uptake of phosphate (nmol) per minute and at 5 minutes the uptake was about 2-fold higher than at 15 minutes and 6-fold higher than the rest of the time points. This data were in agreement with the results obtain in EL-4 cells which makes sense giving the fact that both derive from the same cell type. In both cases, at the first minutes of incubation with radioisotope ^{33}P was the time where the majority of the uptake happened and from 30 minutes on it reached a plateau phase. This indicates that at this point the tracer had nearly equilibrated with the Pi pool inside the cells.

Later on, it was performed a phosphate uptake assay in thymic cells recovered from WT and leukemic mice using two different concentrations of phosphate: 0.32 mM and the positive control (6 mM). In continuity with the assay performed earlier (Figure 3.14A and B) it were used two time-points: 5 and 30 minutes. In the Figure 3.14C is shown the phosphate uptake in WT and leukemic thymic cells after an incubation for 1h with two phosphate conditions. Is evident that when comparing the 0.32 mM Pi condition with the positive control (6 mM), in the first one, the uptake was much lower in both WT and leukemic cells, presenting only residual values of uptake. Apparently, besides the existence or not of a sensing mechanism, cellular uptake depends on the Pi quantity present in the extracellular medium, which deserves further investigation. It is also evident that at the 5 minutes of incubation with the ^{33}Pi radioisotope, the uptake was at its higher rate. This change in the uptake between the different time-points was not observed at the 0.32 mM condition where, with only a residual uptake, there was not enough phosphate to enter in the cell at the first 5 minutes neither there was enough Pi to reach the plateau phase.

In Figure 3.14C there are no differences showed between the uptake in WT and leukemic cells, a factor that would not be expected because carcinogenic cells are known by their abnormal cell growth and enhanced proliferative rate[75] Although it was unexpected, the result in 6 mM, was in agreement with *PCNA* expression (Figure 4.3D) that was lower in leukemic thymic cells. Following the data leukemic cells showed a lower Pi uptake and a lower *PCNA* expression when comparing with WT thymic cells.

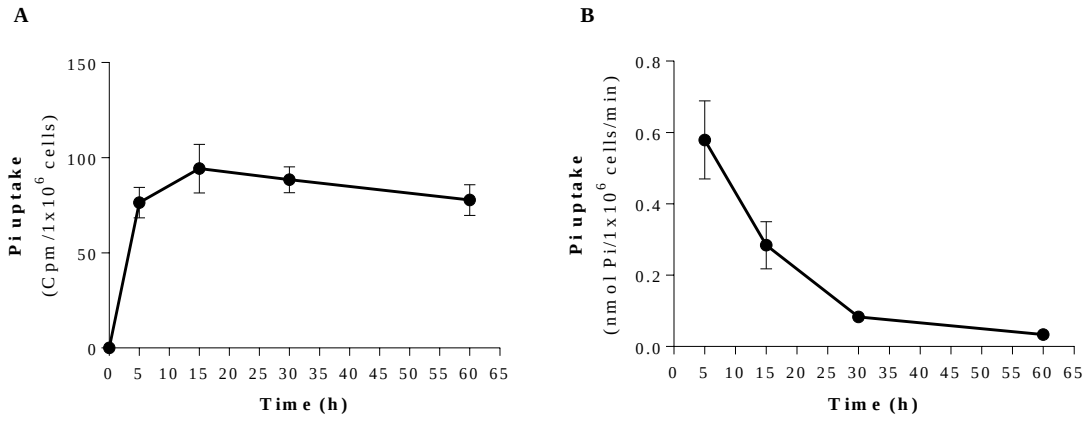

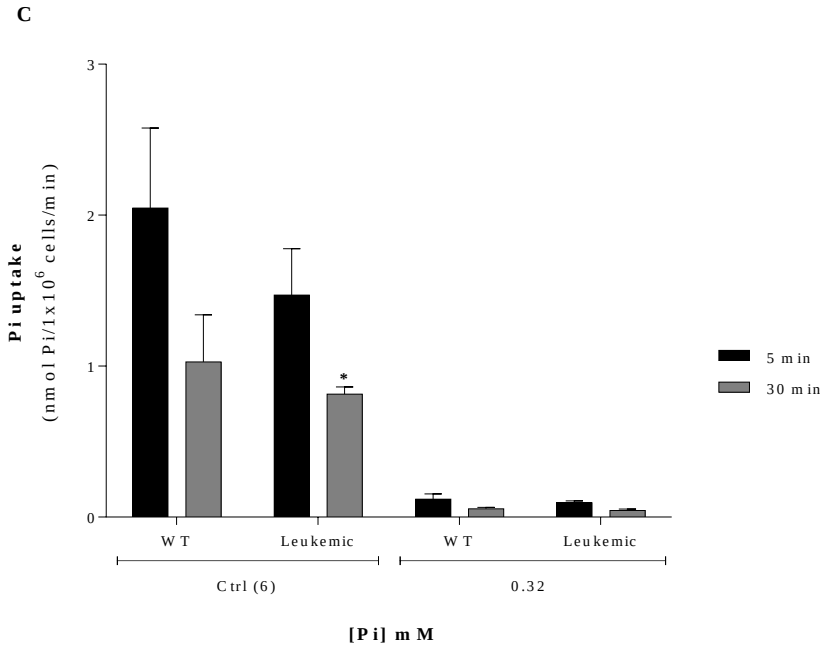

Figure 3.14 – Phosphate uptake in the wild-type and leukemic thymic cells from mice, C57BL/6 strain and TEL-JAK2 transgenic, respectively, under variable phosphate availability. Cells were recovered from a wild-type animal and pre-warmed for 1h at normal conditions, 10% of FBS and 6 mM phosphate. To calculate the Pi uptake over time it were collect 4 samples of $1x10^6$ cells for each time-point (0, 5, 15, 30 and 60 minutes) that cells were incubated with the ^{33}P radioisotope for the Pi uptake measurement. (A) The counts per minute (Cpm) measured by the luminescence counter for each time-point are represented as mean ± SEM (n=2; with 4 technical replicates). (B) The phosphate uptake (nmol) per minute that enter the cell at each time-point is represented as mean ± SEM (n=2; with 4 technical replicates). (C) Cells were recovered from the animals and pre-warmed for 1h with 10% of FBS at two different conditions, 0.32 mM of Pi and using a positive control of 6 mM of Pi. To calculate the Pi uptake in cells after this 1h of incubation, it were collect 4 samples of $1x10^6$ cells from each condition for each time-point (5, and 30 minutes) that the cells were incubated with the ^{33}P radioisotope. The phosphate uptake (nmol) at each time-point is represented as mean ± SEM (n=3 – 5; with 4 technical replicates); *, 0.0265.

4. Conclusion

This study focused on evaluate the role of extracellular phosphate in cell proliferation and the involvement of SLC20 members during this process. Consequently, tissue localization and expression levels of cotransporters PiT-1 and PiT-2, and related genes in mouse model were characterized in an attempt to establish its functional roles and involvement in normal and abnormal cell development and proliferation. It were used a lymphoblastic derived cell line (EL4), and wild-type and leukemic thymic cells removed from mice.

Altogether, the results confirmed the tissues distribution of both SLC20 and SLC34 family described in the literature. Interesting, *XPR1* had an elevated expression in kidney and gastrointestinal tissues, known for an elevated rate of phosphate import and consequently export, supporting its role as Pi exporter. The FBS starvation followed by cell cycle reactivation showed that after 48h, 0.1% FBS cultured cell, enter a quiescent stage that is recovered after the addition of growth factors. These results were reflected in the uptake assay where 0.1% treatment showed a lower Pi uptake. Interestingly, *XPR1* showed an elevated expression in proliferative stages, and *α-klotho*, an aging suppressor, showed the contrary.

Cell proliferation in EL-4 cells, under variable Pi conditions suggested that all the phosphate conditions above or below the positive control (6 mM) resulted in a reduced cell proliferation, although the optimal conditions in human body would be between 1.5 and 3 mM. The uptake assays showed that besides the existence or not of a sensing mechanism, cellular uptake depends on the Pi quantity present in the extracellular medium, which points to a less than perfect modulation of Pi balance. Gene expression in different phosphate conditions over time showed that *PiT-1* and *PiT-2* appear to be important for EL-4 cell proliferation, although their specific role was not investigated. Interestingly, *XPR1* had a high expression, equivalent to *PiT-1* and *PiT-2*. To respond to Pi import seems to be a similar response for Pi export to a response to cellular needs.

It was confirmed the higher number of cells existent in a leukemic thymus comparing with wild-type, although gene expression did not make a reasonable difference, especially proliferating cell marker, *PCNA*, that showed greater expression in wild-type cells but a repetition of this assays is needed to assure this results. Uptake assay only confirmed the results in EL-4 cells, where cellular uptake depends on the Pi quantity present in the extracellular medium.

5. Future work

For future work it would be indicated to repeat and further investigate the gene expression in both FBS and phosphate availability assays, to have certainty in these obtain results.

In addition, it would be indicated as well to perform these cell proliferation, Pi uptake and quantification of the gene expression in other tumorigenic cell lines, established from other tissues, to have a more generalized overview of their role.

Lastly and most important it would be to realize *PiT-1* and *PiT-2* knock-down or knock-out tests in the EL-4 cell line as well in other cell lines. Using these techniques it would be clearer the evaluation of SLC20 family in cell proliferation.

6. Bibliography

1. Berndt T, Kumar R. Novel mechanisms in the regulation of phosphorus homeostasis. *Physiology (Bethesda)*. 2009;24(1):17-25. doi:10.1152/physiol.00034.2008.
2. Berndt TJ. "Phosphatonins" and the regulation of phosphorus homeostasis. *AJP Ren Physiol*. 2005;289(6):F1170-F1182. doi:10.1152/ajprenal.00072.2005.
3. Razzaque MS. The FGF23–Klotho axis: endocrine regulation of phosphate homeostasis. *Nat Rev Endocrinol*. 2009;5(11):611-619. doi:10.1038/nrendo.2009.196.
4. Biber J, Hernando N, Forster I. Phosphate transporters and their function. *Annu Rev Physiol*. 2013;75(1):535-550. doi:10.1146/annurev-physiol-030212-183748.
5. Forster IC, Hernando N, Biber J, Murer H. Phosphate transporters of the SLC20 and SLC34 families. *Mol Aspects Med*. 2013;34(2-3):386-395. doi:10.1016/j.mam.2012.07.007.
6. Giovannini D, Touhami J, Charnet P, Sitbon M, Battini J-L. Inorganic phosphate export by the retrovirus receptor XPR1 in metazoans. *Cell Rep*. 2013;3(6):1866-1873. doi:10.1016/j.celrep.2013.05.035.
7. Virkki L V, Biber J, Murer H, Forster IC. Phosphate transporters: a tale of two solute carrier families. *AJP Ren Physiol*. 2007;293(3):F643-F654. doi:10.1152/ajprenal.00228.2007.
8. Miyamoto K, Segawa H, Ito M, Kuwahata M. Physiological regulation of renal sodium-dependent phosphate cotransporters. *Jpn J Physiol*. 2004;54(2):93-102. doi:10.2170/jjphysiol.54.93.
9. Bian a, Xing C, Hu MC. Alpha Klotho and phosphate homeostasis. *J Endocrinol Invest*. September 2014:1121-1126. doi:10.1007/s40618-014-0158-6.
10. Penido MGMG, Alon US. Phosphate homeostasis and its role in bone health. *Pediatr Nephrol*. 2012;27(11):2039-2048. doi:10.1007/s00467-012-2175-z.
11. Murer H, Forster I, Biber J. The sodium phosphate cotransporter family SLC34. *Pflugers Arch Eur J Physiol*. 2004;447(5):763-767. doi:10.1007/s00424-003-1072-5.
12. Hruska K a, Mathew S, Lund R, Qiu P, Pratt R. Hyperphosphatemia of chronic kidney disease. *Kidney Int*. 2008;74(2):148-157. doi:10.1038/ki.2008.130.
13. Kiela PR, Ghishan FK. Recent advances in the renal-skeletal-gut axis that controls phosphate homeostasis. *Lab Invest*. 2009;89(1):7-14. doi:10.1038/labinvest.2008.114.
14. Bahassi M, Breen GA, Burr JG, et al. Cell Membranes. In: *Medical Cell Biology*. Vol Elsevier; 2008:27-57. doi:10.1016/B978-0-12-370458-0.50007-4.
15. Shaikh A, Berndt T, Kumar R. Regulation of phosphate homeostasis by the phosphatonins and other novel mediators. *Pediatr Nephrol*. 2008;23(8):1203-1210. doi:10.1007/s00467-008-0751-z.
16. Marks J, Debnam ES, Unwin RJ. Phosphate homeostasis and the renal-gastrointestinal axis. *AJP Ren Physiol*. 2010;299(2):F285-F296. doi:10.1152/ajprenal.00508.2009.
17. Bergwitz C, Jüppner H. Phosphate sensing. *Adv Chronic Kidney Dis*. 2011;18(2):132-144. doi:10.1053/j.ackd.2011.01.004.
18. Hediger M a, Clémençon B, Burrier RE, Bruford E a. The ABCs of membrane transporters in health and disease (SLC series): Introduction. *Mol Aspects Med*. 2013;34(2-3):95-107. doi:10.1016/j.mam.2012.12.009.
19. Razzaque MS. FGF23, Klotho and Vitamin D Interactions: In: Vol ; 2012:84-91. doi:10.1007/978-1-4614-0887-1_5.
20. Busch AE, Schuster A, Waldegger S, et al. Expression of a renal type I sodium/phosphate transporter (NaPi-1) induces a conductance in Xenopus oocytes permeable for organic and inorganic anions. *Proc Natl Acad Sci*. 1996;93(11):5347-5351. doi:10.1073/pnas.93.11.5347.

21. Forster I, Hernando N, Sorribas V, Werner A. Phosphate Transporters in Renal, Gastrointestinal, and Other Tissues. *Adv Chronic Kidney Dis*. 2011;18(2):63-76. doi:10.1053/j.ackd.2011.01.006.
22. Murer H, Forster IC, Hernando N, Biber JD. Proximal Tubular Handling of Phosphate. In: *Seldin and Geibisch's The Kidney*. Vol 2. Elsevier; 2013:2351-2368. doi:10.1016/B978-0-12-381462-3.00068-9.
23. Guerreiro PM, Bataille AM, Parker SL, Renfro JL. Active removal of inorganic phosphate from cerebrospinal fluid by the choroid plexus. *Am J Physiol Renal Physiol*. 2014;306(11):F1275-F1284. doi:10.1152/ajprenal.00458.2013.
24. Foster IC, Loo DDF, Eskandari S, Forster IC, Loo DDF, Eskandari S. Stoichiometry and Na binding cooperativity of rat and flounder renal type II Na-P cotransporters. *Am J Physiol*. 1999;276(17):F644-F649. http://www.ncbi.nlm.nih.gov/pubmed/10198426. Accessed May 28, 2015.
25. Forster IC, Biber J, Murer H. Proton-Sensitive Transitions of Renal Type II Na+-Coupled Phosphate Cotransporter Kinetics. *Biophys J*. 2000;79(1):215-230. doi:10.1016/S0006-3495(00)76285-0.
26. SIVAKUMAR G, BATI C, PERRI E, UCCELLA N. Gas chromatography screening of bioactive phytosterols from mono-cultivar olive oils. *Food Chem*. 2006;95(3):525-528. doi:10.1016/j.foodchem.2005.04.003.
27. Biber J, Hernando N, Forster I, Murer H. Regulation of phosphate transport in proximal tubules. *Pflugers Arch Eur J Physiol*. 2009;458(1):39-52. doi:10.1007/s00424-008-0580-8.
28. O'Hara B, Johann S V, Klinger HP, et al. Characterization of a human gene conferring sensitivity to infection by gibbon ape leukemia virus. *Cell Growth Differ*. 1990;1(3):119-127. http://www.ncbi.nlm.nih.gov/pubmed/2078500. Accessed July 15, 2015.
29. Zeijl M, Johann S V, Closs E, et al. A human amphotropic retrovirus receptor is a second member of the gibbon ape leukemia virus receptor family. *Proc Natl Acad Sci U S A*. 1994;91(3):1168-1172. http://www.pubmedcentral.nih.gov/articlerender.fcgi?artid=521475&tool=pmcentrez&rendertype=abstract. Accessed July 15, 2015.
30. Kavanaugh MP, Kabat D. Identification and characterization of a widely expressed phosphate transporter/retrovirus receptor family. *Kidney Int*. 1996;49(4):959-963. http://www.ncbi.nlm.nih.gov/pubmed/8691744. Accessed July 15, 2015.
31. Kavanaugh MP, Miller DG, Zhang W, et al. Cell-surface receptors for gibbon ape leukemia virus and amphotropic murine retrovirus are inducible sodium-dependent phosphate symporters. *Proc Natl Acad Sci U S A*. 1994;91(15):7071-7075. http://www.pubmedcentral.nih.gov/articlerender.fcgi?artid=44340&tool=pmcentrez&rendertype=abstract. Accessed July 3, 2015.
32. Miyamoto KI, Haito-Sugino S, Kuwahara S, et al. Sodium-dependent phosphate cotransporters: Lessons from gene knockout and mutation studies. *J Pharm Sci*. 2011;100(9):3719-3730. doi:10.1002/jps.22614.
33. Shanahan CM, Crouthamel MH, Kapustin A, Giachelli CM. Arterial calcification in chronic kidney disease: Key roles for calcium and phosphate. *Circ Res*. 2011;109(6):697-711. doi:10.1161/CIRCRESAHA.110.234914.
34. Tatsumi S, Segawa H, Morita K, et al. Molecular cloning and hormonal regulation of PiT-1, a sodium-dependent phosphate cotransporter from rat parathyroid glands. *Endocrinology*. 1998;139(4):1692-1699. doi:10.1210/en.139.4.1692.
35. Beck L, Leroy C, Salaün C, Margall-Ducos G, Desdouets C, Friedlander G. Identification of a novel function of PiT1 critical for cell proliferation and independent of its phosphate transport activity. *J Biol Chem*. 2009;284(45):31363-31374.

doi:10.1074/jbc.M109.053132.
36. Beck L, Leroy C, Beck-Cormier S, et al. The phosphate transporter PiT1 (Slc20a1) revealed as a new essential gene for mouse liver development. Lewin A, ed. *PLoS One*. 2010;5(2):e9148. doi:10.1371/journal.pone.0009148.
37. Festing MH, Speer MY, Yang HY, Giachelli CM. Generation of mouse conditional and null alleles of the type III sodium-dependent phosphate cotransporter PiT-1. *Genesis*. 2009;47(12):858-863. doi:10.1002/dvg.20577.
38. Wege S, Poirier Y. Expression of the mammalian Xenotropic Polytropic Virus Receptor 1 (XPR1) in tobacco leaves leads to phosphate export. *FEBS Lett*. 2014;588(3):482-489. doi:10.1016/j.febslet.2013.12.013.
39. Hamburger D. Identification and Characterization of the Arabidopsis PHO1 Gene Involved in Phosphate Loading to the Xylem. *PLANT CELL ONLINE*. 2002;14(4):889-902. doi:10.1105/tpc.000745.
40. Al-Sawan S, Skillen a. W. Phosphate efflux from jejunal enterocytes of the rat: Effect of phosphate concentration gradient and pH. *Cell Biochem Funct*. 1992;10(4):257-260. doi:10.1002/cbf.290100408.
41. Barac-Nieto M, Alfred M, Spitzer A. Basolateral phosphate transport in renal proximal-tubule-like OK cells. *Exp Biol Med (Maywood)*. 2002;227(8):626-631. http://www.ncbi.nlm.nih.gov/pubmed/12192105. Accessed May 28, 2015.
42. Silver J, Naveh-Many T. Phosphate and the parathyroid. *Kidney Int*. 2009;75(9):898-905. doi:10.1038/ki.2008.642.
43. Fukumoto S. Phosphate metabolism and vitamin D. *Bonekey Rep*. 2014;3(February):497. doi:10.1038/bonekey.2013.231.
44. Berndt T, Thomas LF, Craig TA, et al. Evidence for a signaling axis by which intestinal phosphate rapidly modulates renal phosphate reabsorption. *Proc Natl Acad Sci U S A*. 2007;104(26):11085-11090. doi:10.1073/pnas.0704446104.
45. Tanaka Y, Deluca HF. The control of 25-hydroxyvitamin D metabolism by inorganic phosphorus. *Arch Biochem Biophys*. 1973;154(2):566-574. http://www.ncbi.nlm.nih.gov/pubmed/4691503. Accessed August 13, 2015.
46. Sabbagh Y, O'Brien SP, Song W, et al. Intestinal npt2b plays a major role in phosphate absorption and homeostasis. *J Am Soc Nephrol*. 2009;20(11):2348-2358. doi:10.1681/ASN.2009050559.
47. Hattenhauer O, Traebert M, Murer H, Biber J. Regulation of small intestinal Na-P(i) type IIb cotransporter by dietary phosphate intake. *Am J Physiol*. 1999;277(4 Pt 1):G756-G762.
48. Arima K, Hines ER, Kiela PR, Drees JB, Collins JF, Ghishan FK. Glucocorticoid regulation and glycosylation of mouse intestinal type IIb Na-P i cotransporter during ontogeny. *Am J Physiol - Gastrointest Liver Physiol*. 2002;283(2):G426-G434. doi:10.1152/ajpgi.00319.2001.
49. Marks J, Srai SK, Biber J, Murer H, Unwin RJ, Debnam ES. Intestinal phosphate absorption and the effect of vitamin D: a comparison of rats with mice. *Exp Physiol*. 2006;91(3):531-537. doi:10.1113/expphysiol.2005.032516.
50. Bacic D, Schulz N, Biber J, Kaissling B, Murer H, Wagner CA. Involvement of the MAPK-kinase pathway in the PTH-mediated regulation of the proximal tubule type IIa Na+/Pi cotransporter in mouse kidney. *Pflugers Arch*. 2003;446(1):52-60. doi:10.1007/s00424-002-0969-8.
51. Almaden Y, Hernandez A, Torregrosa V, et al. High phosphate level directly stimulates parathyroid hormone secretion and synthesis by human parathyroid tissue in vitro. *J Am Soc Nephrol*. 1998;9(10):1845-1852. http://www.ncbi.nlm.nih.gov/pubmed/9773785. Accessed August 11, 2015.

52. Murer H, Hernando N, Forster I, Biber J. Proximal tubular phosphate reabsorption: molecular mechanisms. *Physiol Rev*. 2000;80(4):1373-1409. doi:1373-1409.
53. Yoshiko Y, Wang H, Minamizaki T, et al. Mineralized tissue cells are a principal source of FGF23. *Bone*. 2007;40(6):1565-1573. doi:10.1016/j.bone.2007.01.017.
54. Urakawa I, Yamazaki Y, Shimada T, et al. Klotho converts canonical FGF receptor into a specific receptor for FGF23. *Nature*. 2006;444(7120):770-774. doi:10.1038/nature05315.
55. Martin A, David V, Quarles LD. Regulation and Function of the FGF23/Klotho Endocrine Pathways. *Physiol Rev*. 2012;92(1):131-155. doi:10.1152/physrev.00002.2011.
56. Perwad F, Azam N, Zhang MYH, Yamashita T, Tenenhouse HS, Portale AA. Dietary and serum phosphorus regulate fibroblast growth factor 23 expression and 1,25-dihydroxyvitamin D metabolism in mice. *Endocrinology*. 2005;146(12):5358-5364. doi:10.1210/en.2005-0777.
57. Chen TH, Kuro-O M, Chen CH, et al. The secreted Klotho protein restores phosphate retention and suppresses accelerated aging in Klotho mutant mice. *Eur J Pharmacol*. 2013;698(1-3):67-73. doi:10.1016/j.ejphar.2012.09.032.
58. Xie B, Chen J, Liu B, Zhan J. Klotho acts as a tumor suppressor in cancers. *Pathol Oncol Res*. 2013;19(4):611-617. doi:10.1007/s12253-013-9663-8.
59. Tan SJ, Smith ER, Hewitson TD, Holt SG, Toussaint ND. The importance of klotho in phosphate metabolism and kidney disease. *Nephrology*. 2014;19(8):439-449. doi:10.1111/nep.12268.
60. Razzaque MS. FGF23-mediated regulation of systemic phosphate homeostasis: is Klotho an essential player? *Am J Physiol Renal Physiol*. 2009;296(3):F470-F476. doi:10.1152/ajprenal.90538.2008.
61. Haussler MR, Whitfield GK, Kaneko I, et al. The role of vitamin D in the FGF23, klotho, and phosphate bone-kidney endocrine axis. *Rev Endocr Metab Disord*. 2012;13(1):57-69. doi:10.1007/s11154-011-9199-8.
62. Kumar R. Phosphate sensing. *Curr Opin Nephrol Hypertens*. 2009;18(4):281-284. doi:10.1097/MNH.0b013e32832b5094.
63. Mouillon JM, Persson BL. New aspects on phosphate sensing and signalling in Saccharomyces cerevisiae. *FEMS Yeast Res*. 2006;6(2):171-176. doi:10.1111/j.1567-1364.2006.00036.x.
64. Markovich D, Verri T, Sorribas V, Forgo J, Biber J, Murer H. Regulation of opossum kidney (OK) cell Na/Pi cotransport by Pi deprivation involves mRNA stability. *Pflügers Arch Eur J Physiol*. 1995;430(4):459-463. doi:10.1007/BF00373881.
65. Segawa H, Kaneko I, Yamanaka S, et al. Intestinal Na-P(i) cotransporter adaptation to dietary P(i) content in vitamin D receptor null mice. *Am J Physiol Renal Physiol*. 2004;287(1):F39-F47. doi:10.1152/ajprenal.00375.2003.
66. Salaün C, Leroy C, Rousseau A, Boitez V, Beck L, Friedlander G. Identification of a novel transport-independent function of PiT1/SLC20A1 in the regulation of TNF-induced apoptosis. *J Biol Chem*. 2010;285(45):34408-34418. doi:10.1074/jbc.M110.130989.
67. Collins JF, Bai L, Ghishan FK. The SLC20 family of proteins: Dual functions as sodium-phosphate cotransporters and viral receptors. *Pflugers Arch Eur J Physiol*. 2004;447(5):647-652. doi:10.1007/s00424-003-1088-x.
68. Tenenhouse HS. Regulation of phosphorus homeostasis by the type iia na/phosphate cotransporter. *Annu Rev Nutr*. 2005;25:197-214. doi:10.1146/annurev.nutr.25.050304.092642.
69. Yoshiko Y, Candeliere GA, Maeda N, Aubin JE. Osteoblast Autonomous Pi Regulation

via Pit1 Plays a Role in Bone Mineralization. *Mol Cell Biol*. 2007;27(12):4465-4474. doi:10.1128/MCB.00104-07.
70. Byskov K, Jensen N, Kongsfelt I, et al. Regulation of cell proliferation and cell density by the inorganic phosphate transporter PiT1. *Cell Div*. 2012;7(1):7. doi:10.1186/1747-1028-7-7.
71. Bøttger P, Pedersen L. Evolutionary and experimental analyses of inorganic phosphate transporter PiT family reveals two related signature sequences harboring highly conserved aspartic acids critical for sodium-dependent phosphate transport function of human PiT2. *FEBS J*. 2005;272(12):3060-3074. doi:10.1111/j.1742-4658.2005.04720.x.
72. Germain RN. T-cell development and the CD4–CD8 lineage decision. *Nat Rev Immunol*. 2002;2(5):309-322. doi:10.1038/nri798.
73. Khanolkar A, Fuller MJ, Zajac AJ. CD4 T Cell-Dependent CD8 T Cell Maturation. *J Immunol*. 2004;172(5):2834-2844. doi:10.4049/jimmunol.172.5.2834.
74. Bushan K, Sharma S, Verma H. A review of thymic tumors. *Indian J Surg Oncol*. 2013;4(2):112-116. doi:10.1007/s13193-013-0214-2.
75. Hanahan D, Weinberg RA. Hallmarks of cancer: the next generation. *Cell*. 2011;144(5):646-674. doi:10.1016/j.cell.2011.02.013.
76. van Meerloo J, Kaspers GJL, Cloos J. Cell sensitivity assays: the MTT assay. *Methods Mol Biol*. 2011;731:237-245. doi:10.1007/978-1-61779-080-5_20.
77. Carron C, Cormier F, Janin A, et al. TEL-JAK2 transgenic mice develop T-cell leukemia. *Blood*. 2000;95(12):3891-3899. http://www.ncbi.nlm.nih.gov/pubmed/10845925. Accessed October 13, 2015.
78. Lacronique V, Boureux A, Valle VD, et al. A TEL-JAK2 fusion protein with constitutive kinase activity in human leukemia. *Science*. 1997;278(5341):1309-1312. http://www.ncbi.nlm.nih.gov/pubmed/9360930. Accessed November 24, 2015.
79. Desjardins P, Conklin D. NanoDrop microvolume quantitation of nucleic acids. *J Vis Exp*. 2010;(45). doi:10.3791/2565.
80. Vandesompele J, De Preter K, Pattyn F, et al. Accurate normalization of real-time quantitative RT-PCR data by geometric averaging of multiple internal control genes. *Genome Biol*. 2002;3(7):RESEARCH0034. http://www.pubmedcentral.nih.gov/articlerender.fcgi?artid=126239&tool=pmcentrez&rendertype=abstract. Accessed July 27, 2014.
81. Werner a, Dehmelt L, Nalbant P. Na+-dependent phosphate cotransporters: the NaPi protein families. *J Exp Biol*. 1998;201(Pt 23):3135-3142.
82. Iyer VR. The Transcriptional Program in the Response of Human Fibroblasts to Serum. *Science (80-)*. 1999;283(5398):83-87. doi:10.1126/science.283.5398.83.
83. Pombinho AR, Laizé V, Molha DM, Marques SMP, Cancela ML. Development of two bone-derived cell lines from the marine teleost Sparus aurata; evidence for extracellular matrix mineralization and cell-type-specific expression of matrix Gla protein and osteocalcin. *Cell Tissue Res*. 2004;315(3):393-406. doi:10.1007/s00441-003-0830-1.
84. Zarubin T, Han J. Activation and signaling of the p38 MAP kinase pathway. *Cell Res*. 2005;15(1):11-18. doi:10.1038/sj.cr.7290257.
85. Wajant H, Pfizenmaier K, Scheurich P. Tumor necrosis factor signaling. *Cell Death Differ*. 2003;10(1):45-65. doi:10.1038/sj.cdd.4401189.
86. Sabatino DE, Do B-KQ, Pyle LC, et al. Amphotropic or Gibbon Ape Leukemia Virus Retrovirus Binding and Transduction Correlates with the Level of Receptor mRNA in Human Hematopoietic Cell Lines. *Blood Cells, Mol Dis*. 1997;23(3):422-433. doi:10.1006/bcmd.1997.0161.

Appendix

Annex 1: Solutions

DEPC water

For 2 liters: A volume of 200 µL of diethylpyrocarbonate (DEPC) was added to 2 L of distilled water in a dark glass bottle. The mixture was agitated and left to rest for 24 h before autoclaved.

Loading buffer

Prepare a solution of 40% glucose in sterile water (40 g of glucose in 100 ml). When the glucose was dissolved was added a small amount of bromophenol blue, just to give some color to the solution. The solution was filter sterilize with a syringe coupled to an adapter filter of 0.2 µm, aliquoted and stored at -20ºC.

Phosphate-buffered saline (PBS) 10x

For 1 liter of milliQ water was added:

- 80 g of sodium chloride (NaCl);
- 2 g of potassium chloride (KCl);
- 18,05 g of sodium phosphate monobasic ($NaH_2PO_4.H_2O$);
- 2,4 g of potassium dihydrogen phosphate (KH_2PO_4);

The solution was filter sterilize with a filter unit adapted with a filter of 0.2 µm and stored at room temperature.

$NaHCO_3$ solution 0.6 M

Dissolve 0.5 g in 10 mL of distilled water. The solution was filter sterilize with a filter unit adapted with a filter of 0.2 µm and stored at RT.

Phosphate Sorensen buffer 0,5M

Stock solution A: 0.5 M potassium dihydrogen phosphate (KH_2PO_4).
Dissolve 0.68 g KH_2PO_4 in 10 mL distilled water.
Stored at 4ºC.

Stock solution B: 0.5 M disodium hydrogen phosphate ($Na_2HPO_4.2H_2O$).
Dissolve 1.78 g $Na_2HPO_4.2H_2O$ in 20 mL distilled water.
Stored at RT.

To obtain a solution at pH 7.7 (the same pH of the culture medium to were this solution was added) it was mixed 2 mL of solution A to 8 mL of solution B. The solution was filter sterilize with a filter unit adapted with a filter of 0.2 µm and stored at 4ºC.

Annex 2: Alignments of the sequenced fragment with the original mRNA sequence obtained from NCBI (http://www.ncbi.nlm.nih.gov)

NaPi-IIa

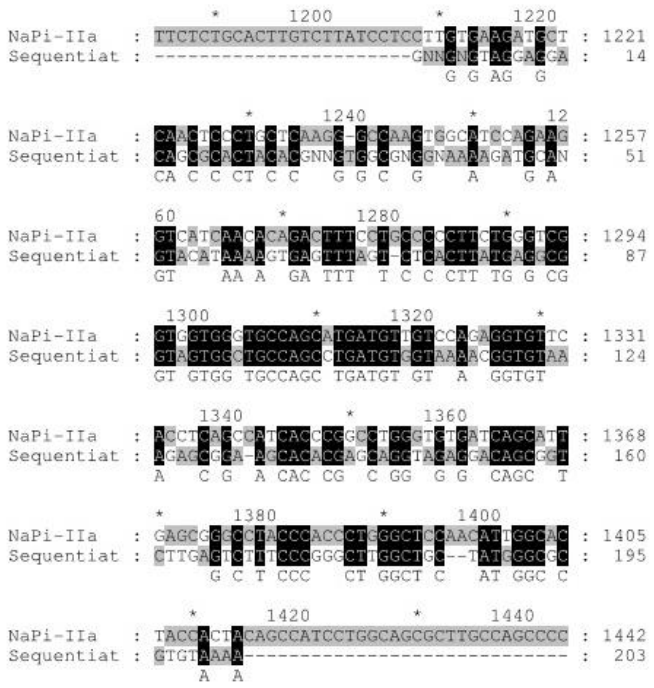

Figure 6.1 – Clustal X2 alignment of the sequence from the database NCBI and the NaPi-IIa RT-PCR amplicon sequence submitted to sequencing.

NaPi-IIb

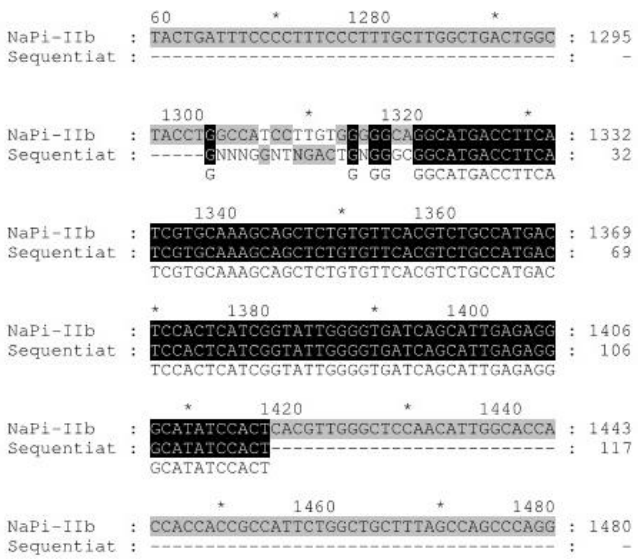

Figure 6.2 – Clustal X2 alignment of the sequence from the database NCBI and the NaPi-IIb RT-PCR amplicon sequence submitted to sequencing.

PiT-1

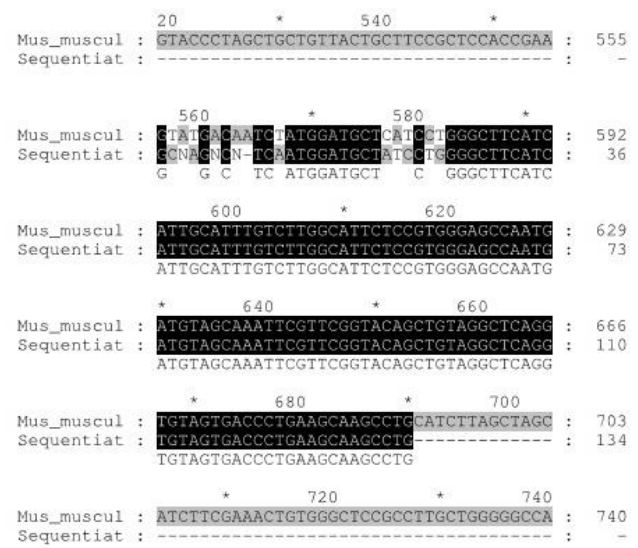

Figure 6.3 – Clustal X2 alignment of the sequence from the database NCBI and the PiT-1 RT-PCR amplicon sequence submitted to sequencing.

PiT-2

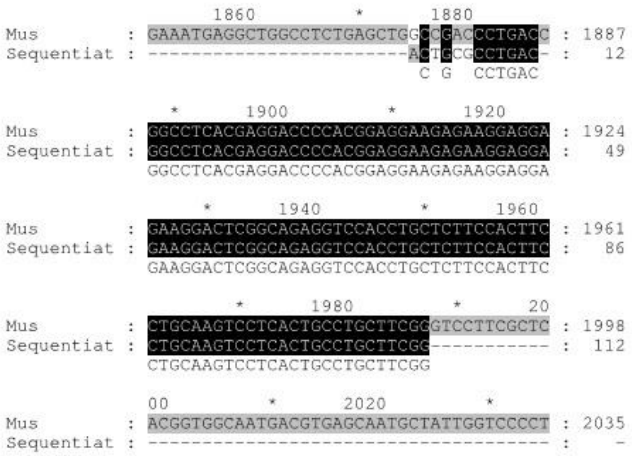

Figure 6.4 – Clustal X2 alignment of the sequence from the database NCBI and the PiT-2 RT-PCR amplicon sequence submitted to sequencing.

α-Klotho

Figure 6.5 – Clustal X2 alignment of the sequence from the database NCBI and the α-Klotho RT-PCR amplicon sequence submitted to sequencing.

XPR1

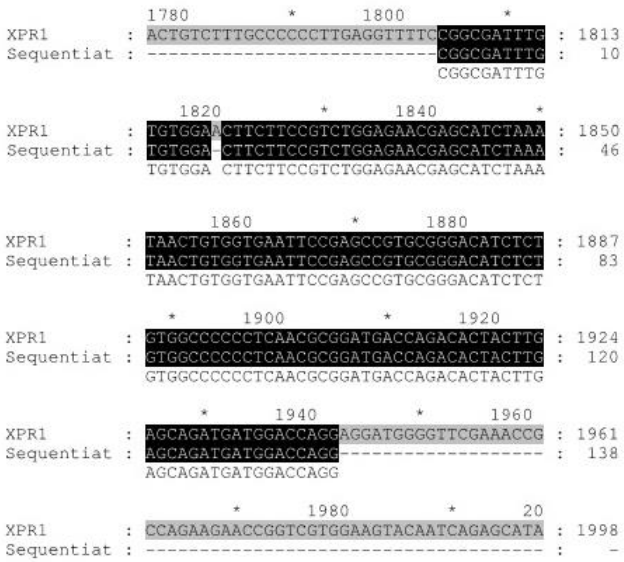

Figure 6.6 – Clustal X2 alignment of the sequence from the database NCBI and the XPR1 RT-PCR amplicon sequence submitted to sequencing.

PCNA

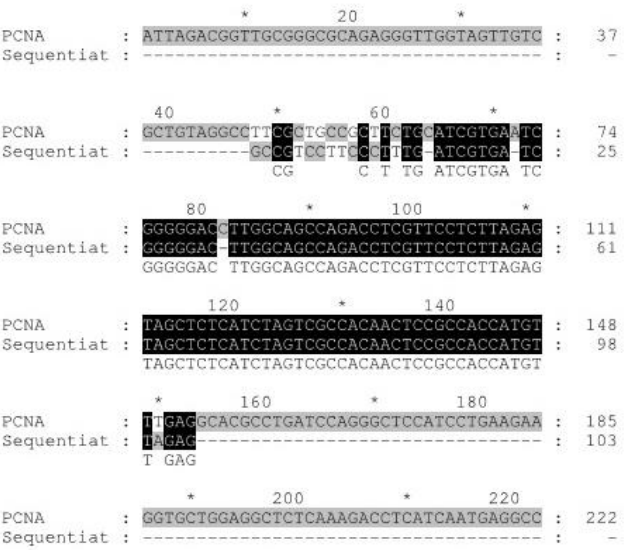

Figure 6.7 – Clustal X2 alignment of the sequence from the database NCBI and the PCNA RT-PCR amplicon sequence submitted to sequencing.

18S

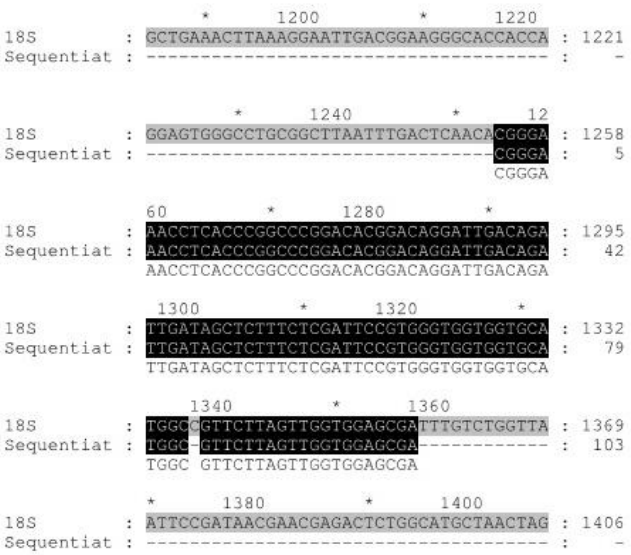

Figure 6.8 – Clustal X2 alignment of the sequence from the database NCBI and the XPR1 RT-PCR amplicon sequence submitted to sequencing.